Wave Propagation in Ray-Chaotic Enclosures: Paradigms, Oddities and Examples

Vincenzo Galdi[1], Innocenzo M. Pinto[1], and Leopold B. Felsen[2]

[1]Waves Group, Department of Engineering, University of Sannio
Palazzo Dell'Aquila Bosco-Lucarelli, Corso Garibaldi 107
I-82100 Benevento, Italy
Tel: +39 0824 305809; Fax: +39 0824 305840; E-mail: vgaldi@unisannio.it, pinto@sa.infn.it

[2]Dept. of Aerospace & Mechanical Engineering and Dept. of Electrical & Computer Engineering
Boston University, 110 Cummington St., Boston MA 02215 USA (part-time)
also, University Professor Emeritus, Polytechnic University, Brooklyn, NY, USA
Tel: +1 (617) 353-4939; Fax: +1 (617) 353-5866; E-mail: lfelsen@bu.edu

Abstract

Ray chaos, characterized by eventual exponential divergence of originally nearby multi-bounce ray trajectories, is an intriguing phenomenon. It can be observed in several electromagnetic wave propagation scenarios: both *very complex* (e.g., urban areas) and *very simple* (e.g., a stadium-shaped cavity) scenarios. This paper contains a compact review of known results on wave propagation in ray-chaotic scenarios. Attention is focused principally on two-dimensional simple paradigms of *internal* ray chaos ("ray-chaotic billiards"), with emphasis on possible implications for high-frequency *wave* dynamics ("ray-chaotic footprints"). General concepts, tools, and numerical examples are discussed, and their potential relevance to current challenges in electromagnetic engineering is noted.

Keywords: Chaos; cavity resonators; propagation; geometrical optics; geometrical theory of diffraction; reverberating enclosures

The hidden harmony is better than the obvious.

Heraclitus of Ephesus

1. Introduction

For centuries, scientists and engineers have focused most of their attention on the "realm of linear models," where systems are gracefully predictable, and have looked at the extremely complex and disordered dynamics of natural phenomena, such as weather evolution, fluid turbulence, etc., as *disturbing exceptions*. However, starting from the 1970s, scientists from different disciplines began looking at *complexity* and *disorder* from a different perspective, with a growing awareness that *extremely simple* nonlinear mathematical models can give rise to *extremely complex* and *rich* dynamics, with *order* and *disorder* side-by-side. In 500 BC, the Greek philosopher Heraclitus had imagined a scenario where each component of the world had its own counterpart, with these opposing forces interplaying permanently within the great eternal movement, thereby exhibiting *harmony* and *chaos* (from the Greek word *Khaos*, meaning "gaping void"). About 2500 years later, the mathematical foundations were finally being laid for his perception, leading to the development of an entirely new multidisciplinary science, now known as "chaos" or, more precisely, "deterministic chaos." The reader is referred to classic textbooks and review articles such as [1-3] for an introduction and review concerning this subject area. A brief introduction is also provided in Appendix A.

Technically, the term "deterministic chaos" is used to indicate exponential sensitivity – in the evolution of an even weakly *nonlinear* dynamical system – to initial conditions, resulting in long-time algorithmic unpredictability and random-like behavior. This is often exemplified via the so-called "butterfly effect," i.e., a butterfly flapping its wings in Brazil causing a tornado in Texas. Interestingly, when scientists started looking for chaos, chaos appeared to be hidden *almost everywhere* in nature, ranging from the beating heart to the stock market. However, it was not until the last fifteen years that it was recognized as a powerful engineering tool (see [4]), far from being a mere mathematical oddity of purely academic interest.

One of the most thought-provoking issues is related to *ray chaos*, i.e., eventual exponential divergence of multi-bounce, originally nearby, coincident rays in *strictly deterministic* orderly environments. The study of ray-chaotic boundary-value problems (BVPs) poses a variety of fundamental and challenging wave-

 ISSN 1045-9243/2005/$20 ©2005 IEEE

theoretic and modeling issues. In this connection, simple paradigms can be obtained via analogies with mechanical "billiards" (see Section 3). Despite their deceptively *simple* geometric/constitutive features, ray-chaotic "billiard" enclosures may exhibit fairly *complex* electromagnetic (EM) responses, thereby raising the question of whether ray chaos may be hidden within the corresponding *wave* (i.e., *finite* wavelength) dynamics. At first glance, this question seems to be a contradiction in terms, since it implies reconciliation of the extremely *complex* and *irregular* features of chaos with the *inherently smooth* character of wave dynamics. However, there is substantiated evidence that ray-chaotic systems, when observed in the short (but *finite*) wavelength regime, exhibit features that differ considerably from those associated with "regular" ray behavior. Ray chaos therefore seems capable of impressing *clear*, and often *universal*, "footprints" on the high-frequency wave dynamics; this is the subject of *wave/quantum chaology* [5, 6]. Although most available investigations on the subject (both theoretical and experimental) are set in a quantum physics framework (classical versus quantum chaos, see [5, 6] for a review), the main results and conclusions are *general* and apply to all kinds of wave phenomena. However, due to the use of different terminology, these results have most likely not come to the attention of most researchers in applied EM.

This paper is an attempt to summarize the subject in a simple and hopefully palatable form, with quantitative discussion of only a few technical issues, and details relegated to a comprehensive list of selected relevant references. Attention is focused on examples and results pertaining to two-dimensional (2D) closed billiards. It is our intent to motivate the reader to further explore this subject, which is not only appealing but may have potentially interesting applications in EM engineering (see the discussion in Section 6). Accordingly, the contents of the paper are organized as follows. Section 2 presents a brief review of EM-related chaotic phenomena and applications. Section 3 deals with the ray analysis in regular and ray-chaotic "billiard" enclosures. Section 4 contains a review of the basic concepts and tools from "wave chaology," citing known results on ray-chaotic footprints in deterministic wave dynamics. Section 5 deals with a *new* numerical example of *pulsed* EM propagation in ray-chaotic enclosures. Section 6 presents conclusions, perspectives, and open issues. A few technical considerations are collected in Appendices A and B. Specifically, chaos basics are summarized in Appendix A, whereas a nomenclature of systems in order of increasing complexity is provided in Appendix B. The representative bibliography cited in the text is supplemented by an ordered comprehensive list of references for better appreciation of the scope of this subject area.

2. Electromagnetic Chaos

2.1 Classic Paradigms

The simplest conceivable paradigms of true (i.e., inherently nonlinearity induced) EM chaos are probably those featuring circuit (voltage versus current) nonlinearities, e.g., a transmission line loaded by a Chua circuit [7]. Nonlinear material constitutive properties, especially at optical frequencies, play a similar role in inducing chaos (see [8] for a review). However, even in *linear* media, chaos can occur as an effect of *nonlinear coupling* between mechanical and EM degrees of freedom, as in Fabry-Perot resonators with (freely swinging, heavy) pendular mirrors [9].

It should be emphasized that in most practical applications, chaos is actually an *unwanted* source of instability, whence the main motivation for investigating its possible onset is learning the rules for avoiding it. However, in some applications, one *intentionally* seeks evolution to chaos. Recent advances in chaos synchronization [10] have suggested the exploration of "chaotic waveforms" as a tool for scrambling/unscrambling signals in EM-based secure communication systems [11].

2.2 Ray Chaos

As noted earlier, ray chaos implies eventual *exponential* separation of nearby-originating multi-bounce *ray trajectories*. Even in *linear* EM systems, ray-chaotic behavior can be induced by certain geometrical features of reflecting boundaries (e.g., focusing/defocusing), as well as by constitutive ray-trapping properties of the medium. This is in view of the *inherent nonlinearity* of the *ray-tracing maps* governed by the (nonlinear) eikonal equation, $(\nabla\varphi)^2 = n^2$, where φ is the ray phase and n is the refractive index. Remarkably, such complex behavior may be observed in relatively simple scenarios, and instructive paradigms of EM ray chaos can be envisaged by exploiting formal analogies between ray optics and classical (particle) mechanics. In this connection, the simplest paradigms are provided by "billiards," i.e., closed homogeneous domains wherein an internally-launched point particle (ray) moves freely, subject only to specular (reflected) bounces at each encounter with the boundary (see Section 3).

On the practical side, ray chaos has been demonstrated to play a key role in several EM and acoustic applications. In particular, ray-chaotic models have been applied successfully to the characterization of complex radar signatures [12] and to the analysis and design of reverberating enclosures (see Section 2.3). Also, unusual effects have been found in connection with optical and photonic technology, leading to the development of the bowtie solid-state micro-laser [13]. This device, based on the use of an oval-shaped ray-chaotic dielectric resonator, is probably the most popular technological application of ray chaos to date (see also the Web site maintained by J. U. Nöckel at the University of Oregon [14]).

2.3 Chaos in Reverberating Enclosures

Electromagnetic reverberation enclosures (EREs) are well-known standard tools for *narrowband* EM compatibility/interference testing [15]. Besides their practical interest, they provide a nicely viable paradigm of the multi-faceted connections between deterministic models, complex systems, chaos, and stochastic behavior.

In [16], a simple two-dimensional ray model of (mechanically) mode-stirred electromagnetic reverberation enclosures was introduced. This showed that the spatial field homogenization with Rayleigh-like field-intensity distribution in time, observed in electromagnetic reverberation enclosures [17], can be related to the onset of chaos as the peak-to-peak displacement of the mode-stirring wall becomes comparable to the EM field wavelength. Remarkably, the simple model in [16] turns out to reproduce experimentally observed electromagnetic- reverberation-enclosure features, and sheds light on the underlying physics, suggesting conceptual foundations of the well known thermodynamic electromagnetic-reverberation-enclosure theory [18]. Moreover, it allows for synthetic assessment of electromagnetic-reverberation-

enclosure performance in terms of Lyapounov exponents [1-3] (see also Appendix A), and provides *quantitative* design criteria.

Our interest in ray chaos originated within this framework. It was initially motivated by the hope that *pulsed* (wideband) reverberating (multi-echoing) operation could be obtained in *ray-chaotic* enclosures, where, under suitable conditions, an initially localized electromagnetic wave-packet would eventually generate a nearly-uniform and isotropic "pulse shower." This could illuminate the equipment under test in a fashion largely independent of the target's location, orientation, shape, and electrical constitutive properties. The encouraging *new* results obtained within the limits of a simple ray analysis [19] suggested an investigation of the *general* properties of wave dynamics in ray-chaotically-inclined enclosures versus enclosures with regular (non-chaotic) features. The extent to which this picture is complicated in a full-wave analysis will be further discussed in Section 5.

3. Ray Analysis: Regular Versus Chaotic Internal Billiards

The simplest EM "billiard" prototype is defined as a perfectly conducting enclosure filled with a homogeneous medium, wherein ray paths are straight lines subject to specular reflection (where the incidence angle is equal to the reflection angle) at the boundary.

A gallery of two-dimensional, regular, pseudo-regular, and ray-chaotic billiard prototypes is shown in Figure 1. Examples of regular billiards include rectangular (Figure 1a) and elliptical (Figure 1b) geometries. Generally speaking, billiards in *coordinate-separable* geometries are characterized by *completely integrable* dynamics (see Appendix B for terminology), i.e., they give rise to *regular* ray trajectories. Polygonal billiards, like that in Figure 1c, are generally *neither chaotic nor integrable*. Rational polygonal billiards (i.e., with all angles rationally related to π) are typically referred to as "pseudo-integrable." Notable exceptions (besides the already mentioned rectangles) are the equilateral triangles, the $\pi/2-\pi/4-\pi/4$ triangles, and the $\pi/2-\pi/3-\pi/6$ triangles, which are examples of *non-separable* geometries with *regular* ray dynamics. While billiards with *defocusing* walls – which increase the separation between nearby trajectories – can intuitively be expected to exhibit ray chaos, some billiards with *focusing* walls (e.g., the stadium in Figure 1d) likewise exhibit ray chaos [3]. Other examples of ray-chaotic billiards include the D-shaped truncated circle (Figure 1e), and the so-called Sinai billiard (Figure 1f). These ray-chaotic billiards share the property of admitting at least one (albeit unstable) closed ray trajectory (K-systems, in the terminology of Appendix B). In the stadium billiard, for instance, there exist several (stable and unstable) closed ray trajectories, the most trivial being those bouncing vertically between the straight parallel walls. An example of a ray-chaotic billiard without any closed ray trajectory (a C-system, in the terminology of Appendix B) is given by the geometry in Figure 1g, the boundary of which is formed by four intersecting circles with non-commensurate radii, with centers lying on two skew lines. Note that from the ray-chaotic geometries in Figures 1d-1f, *regular* billiards can be obtained as limiting cases (e.g., reducing the straight segments in Figures 1d and 1e, or the circle radius in Figure 1f, to zero). Although not of direct interest in this paper, also shown in Figure 1 are two prototypes of *open* chaotic billiards: the so-called "three-disk pinball" (Figure 1h), and the gravitational billiard in Figure 1i, where a heavy point mass (subject to gravity) bounces onto a periodic perfectly-reflecting boundary. The reader is referred to [20] and [21] where the EM counterparts of these two systems were investigated.

The completely different sensitivities with respect to initial conditions for regular and ray-chaotic billiards are illustrated in Figure 2. Two ray trajectories (displayed in red and blue), originating from the same point (the center of the billiard), but with launch angles differing by 0.001°, were traced up to 15 boundary reflections. In the regular (rectangular) billiard (Figure 2a), they remained practically indistinguishable, whereas in the ray-chaotic (stadium) billiard (Figure 2b), their rapid splitting-apart was evident.

Typical space-filling properties of ray trajectories in regular billiards are exemplified in Figure 3. In rectangular billiards, the ray trajectories may either form a *regular, closed* mesh when the launch angle belongs to the (countable) infinite set corresponding to the geometrical resonances (Figure 3a), or they may fill the whole billiard in a *regular* (checkerboard) fashion, without closing at all (Figure 3b). In circular billiards, periodic trajectories are possible, as well (Figure 3c), as are the regular annular-sector-filling trajectories, bounded by a circular caustic (Figure 3d). In elliptic billiards, apart from possible periodic trajectories (not shown), rays tend to fill the billiard area confined by either *elliptic* or *hyperbolic* caustics, as exemplified in Figures 3e and 3f, respectively. As the rays fill up the billiard enclosure (in Figure 3, only 300 reflections are shown for the non-periodic trajectories), it becomes difficult to keep track of the ray bounces and their possible regular/irregular behavior. In this connection, it is instructive and insight-providing to look at diagrams in the configuration-spectrum phase space. For

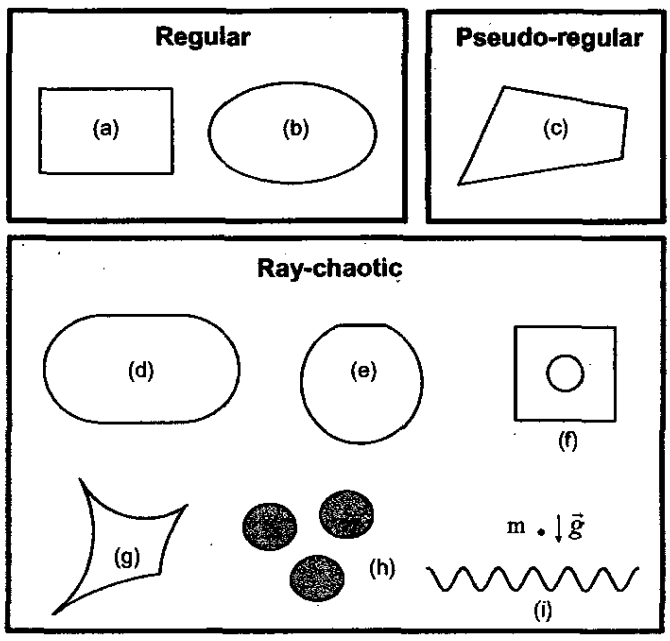

Figure 1. Examples of two-dimensional regular, pseudo-regular, and ray-chaotic billiards. Regular billiards: (a) rectangular, (b) elliptic. Pseudo-regular billiard: (c) polygonal. Ray-chaotic billiards: (d) stadium, (e) cut-circle (with the straight cut not corresponding to a diameter), (f) Sinai, (g) billiard formed by four intersecting circles with non-commensurate radii the centers of which lie on two skew lines, (h) "three-disk pinball," (i) gravitational billiard where a heavy point mass (subject to gravity) bounces onto a periodic perfectly reflecting boundary.

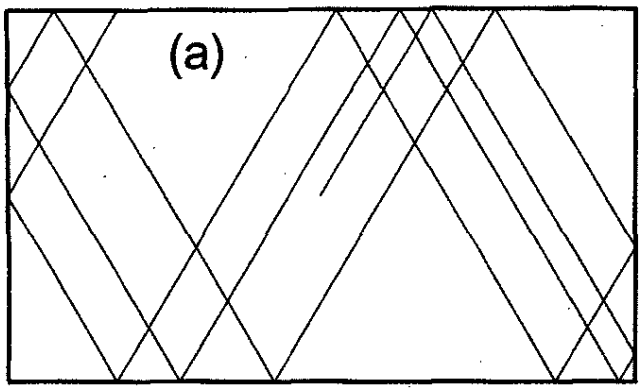

Figure 2a. An illustration of sensitivity with respect to initial conditions in regular and ray-chaotic billiards. Two ray trajectories (displayed in red and blue) originating from the same point (the center of the billiard), but with launch angles differing by 0.001°, are evolved up to 15 boundary reflections. For the rectangular billiard (regular), the two trajectories are practically indistinguishable.

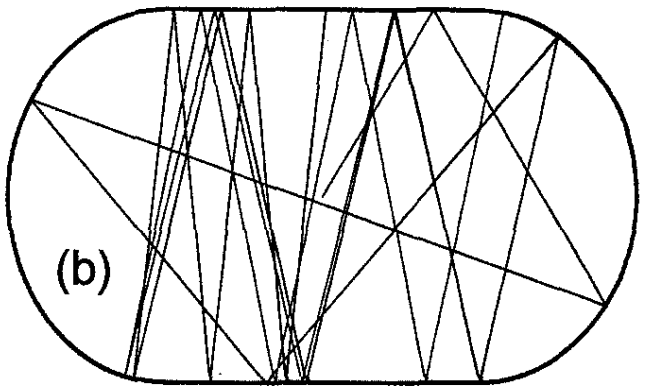

Figure 2b. An illustration of sensitivity with respect to initial conditions in regular and ray-chaotic billiards. Two ray trajectories (displayed in red and blue) originating from the same point (the center of the billiard), but with launch angles differing by 0.001°, are evolved up to 15 boundary reflections. For the stadium billiard (ray-chaotic), the two trajectories start diverging and become widely separated after a few bounces.

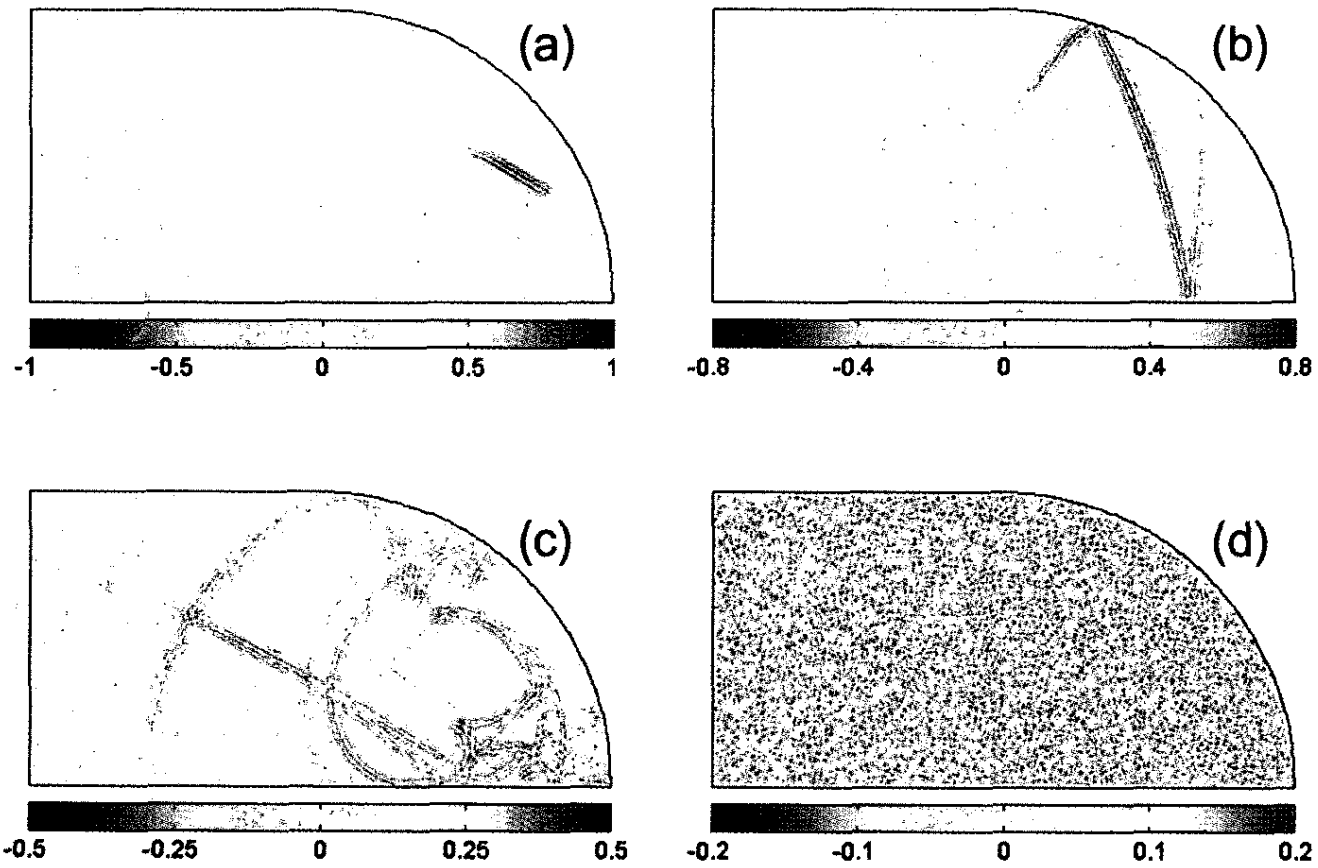

Figure 10. Instantaneous snapshots of the field distribution, displaying the progressive spreading of the initially localized wave packet, eventually covering the entire enclosure. The geometry and parameters were as in Figure 9. (a) $t = 3T$, (b) $t = 40T$, (c) $t = 100T$, (d) $t = 1000T$.

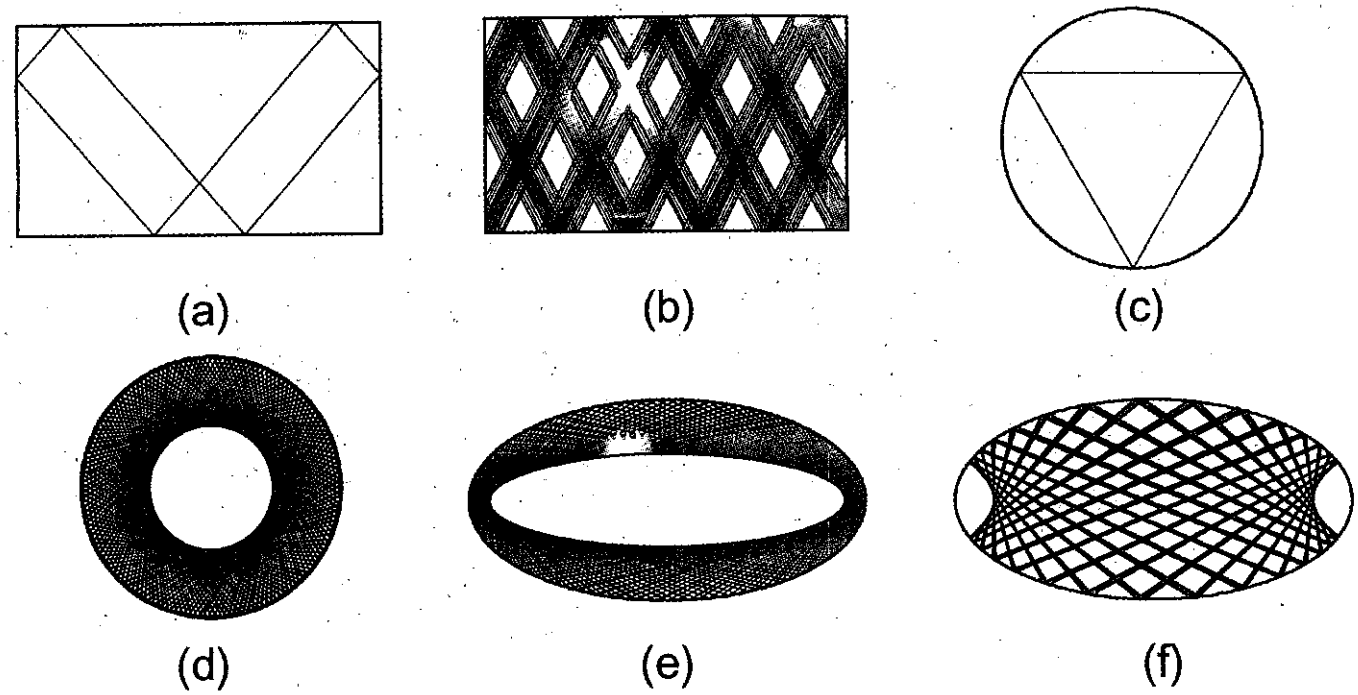

Figure 3. An illustration of the space-filling properties of ray trajectories in regular billiards: (a) a rectangular billiard with a periodic trajectory, (b) a space-filling trajectory (300 reflections) with a checkerboard pattern, (c) a circular billiard with a periodic trajectory, (d) a space-filling trajectory (300 reflections) displaying a circular caustic, (e) an elliptic billiard with a space-filling trajectory (300 reflections) displaying an elliptic caustic, (f) a space-filling trajectory (300 reflections) displaying a hyperbolic caustic.

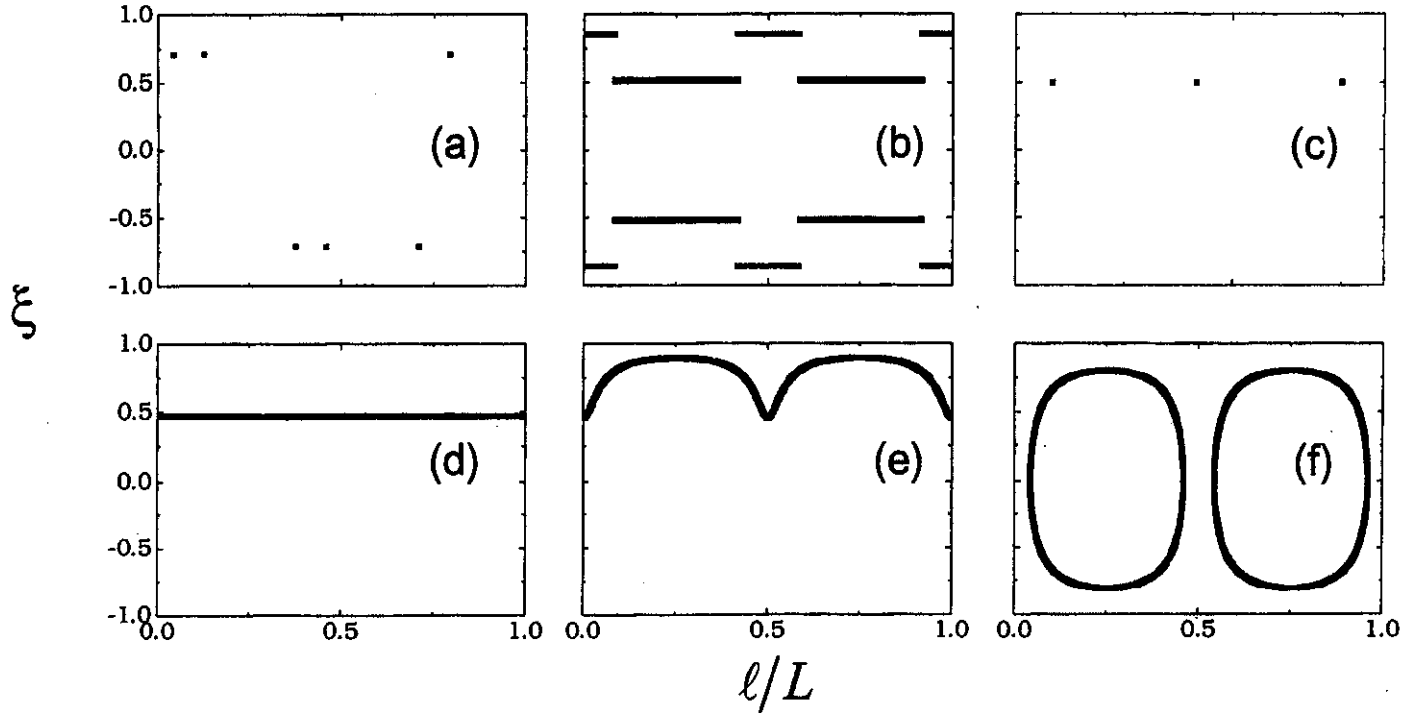

Figure 4. Phase-space diagrams pertaining to the trajectories in Figure 3. Each point in the diagram corresponds to a reflection point, the position of which is parameterized in terms of the curvilinear abscissa, ℓ (scaled by the billiard perimeter, L), measured along the billiard boundary in the counterclockwise sense from its right intersection with the horizontal symmetry axis. The spectral variable, ξ, on the ordinate denotes the cosine of the departure angle, α, with respect to the local tangent unit vector. For the non-periodic ray trajectories, 10^4 reflections were included. In all cases, the phase-space diagrams are either finite sets of points or smooth curves.

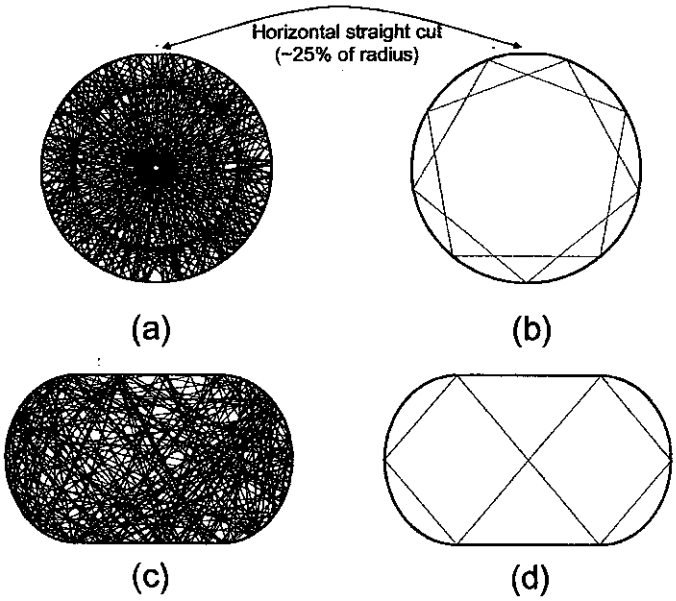

Figure 5. An illustration of the space-filling properties of ray trajectories in ray-chaotic billiards. Cut-circle billiard (as in Figure 1e, with a horizontal straight cut ~25% of the radius): (a) Uniformly space-filling chaotic trajectory (1000 reflections); (b): Marginally stable periodic trajectory. Stadium billiard: (c) Uniformly space-filling chaotic trajectory (1000 reflections); (d) Unstable periodic trajectory.

each reflection, typical phase-space diagrams display the impact-point position versus the angle of departure of the reflected ray. In Figure 4, such diagrams are shown for the trajectories in Figure 3. The reflection position is parameterized in terms of the curvilinear abscissa, ℓ (scaled by the billiard perimeter, L), measured along the billiard boundary in the counterclockwise sense from its right intersection with the horizontal-symmetry axis. The spectral variable, $\xi = \cos\alpha$, on the ordinate denotes the cosine of the departure angle, α, with respect to the local unit vector tangent to ℓ. For the non-periodic ray-trajectories, 10^4 reflections were included. Apart from the simplest point mapping of the periodic trajectories in Figures 3a and 3c in the phase space (Figures 4a and 4c), the smooth phase-space diagrams in Figures 4b, 4d, 4e, and 4f clearly highlight the inherent *regularity* of the corresponding space-filling trajectories in Figures 3b, 3d, 3e, and 3f.

Examples of ray trajectories in chaotic billiards and their phase space diagrams are shown in Figures 5 and 6, respectively. Figure 5a shows a trajectory with the same initial conditions as in Figure 3d, but encountering the horizontal straight cut (~25% of the radius) in the circle (the cut-circle billiard in Figure 1e). Although hardly visible on the scale of the plot, the small straight cut dramatically affects the ray dynamics. The circular caustic in Figure 3d has now disappeared, and the rays tend to fill up the entire billiard in a very irregular fashion. This visual impression is confirmed by the corresponding phase-space diagram in Figure 6a, which now displays a practically *uniform* filling of the phase space (instead of the *single* spectral line in Figure 4d). In general, for

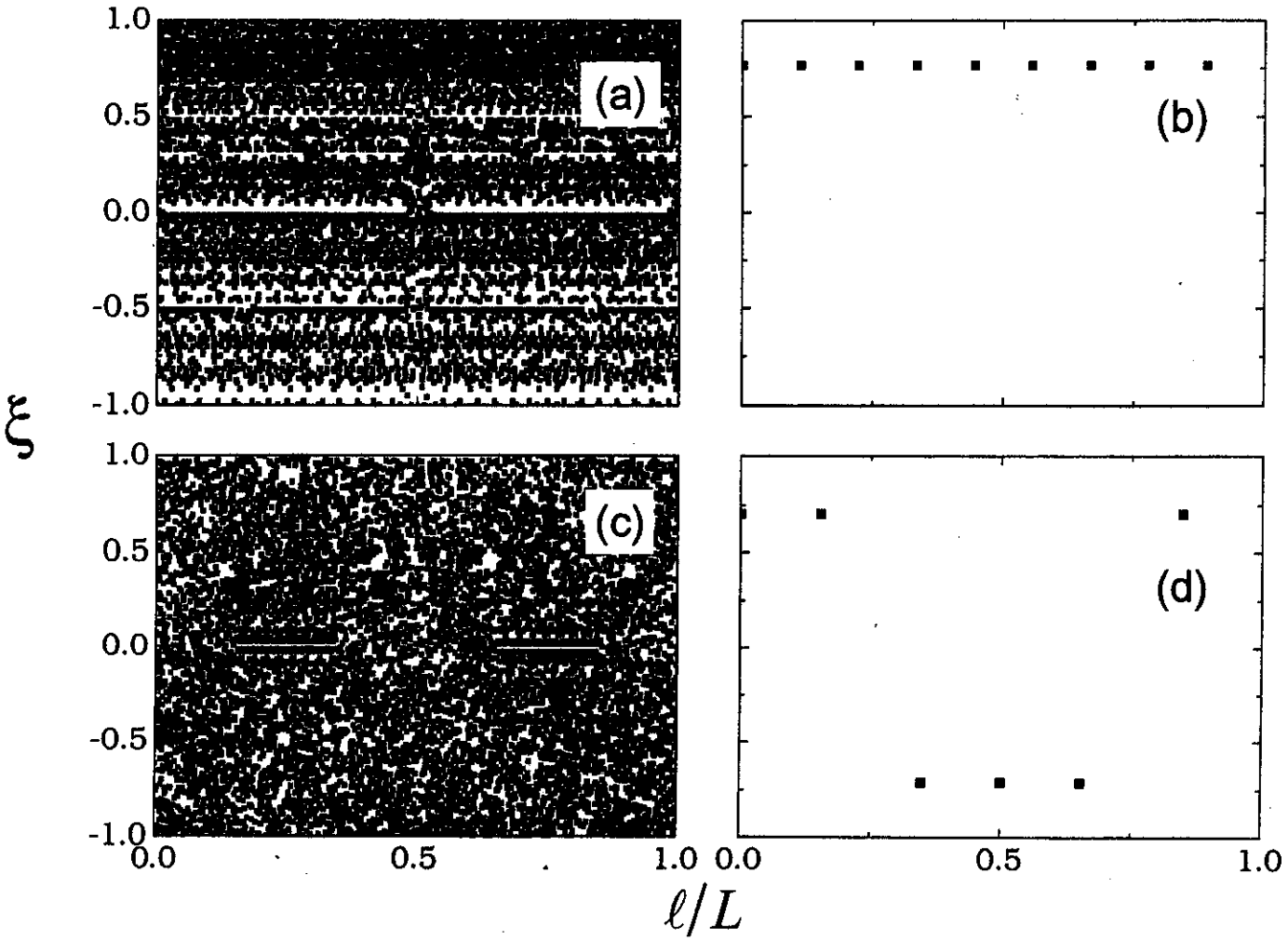

Figure 6. Phase-space diagrams pertaining to the trajectories in Figure 5. For the chaotic trajectories (a) and (c), the phase space is uniformly covered asymptotically (10^4 reflections shown).

ray-chaotic billiards (asymptotically, as the number of reflections approaches infinity), the phase space is covered uniformly by almost any ray trajectory, and exhibits "regular islands" (represented, e.g., by non-isolated, marginally stable, closed trajectories) amid a "chaotic sea" [3]. For the billiard in Figure 1e, a typical non-isolated marginally stable closed trajectory is shown in Figure 5b, with the corresponding phase-space diagram displayed in Figure 6b. Similar features are observed in the stadium billiard of Figure 1d. Specifically, Figures 5c and 6c show the evolution of a typical chaotic trajectory and the corresponding phase-space diagram, respectively. An example of an isolated unstable periodic trajectory and the corresponding phase-space diagram are shown in Figures 5d and 6d, respectively.

To sum up, in regular billiards, ray trajectories tend to fill the billiard area in a regular fashion, with arrival directions spatially distributed according to *smooth* phase-space relationships. Conversely, in chaotic billiards, ray trajectories (apart from possible zero-measure sets of initial conditions) tend to cover the billiard *ergodically* (in the terminology of Appendix B), approaching almost every point in the billiard arbitrarily closely, arbitrarily many times, with uniformly distributed arrival angles.

4. Ray-Chaotic Footprints: A Review

4.1 Background

As noted in the introduction, although the wave dynamics in ray-chaotically-inclined deterministic boundary-value problems (BVPs) is *strictly non-chaotic*, one can anticipate "ray-chaotic footprints" in the high-frequency regime, with the wavelength setting a scale beyond which "complexity" cannot be further resolved. These "ray-chaotic footprints" relate to distinctive features in the wave dynamics that are not exhibited by boundary-value problems featuring regular ray behavior. The wave dynamics of ray-chaotic "billiard" enclosures has been thoroughly investigated, both theoretically and experimentally, in quantum physics, in connection with *classical* versus *quantum* chaos (see [5, 6] for a review). Most available results pertain to the high-frequency analysis of the steady-state Schrödinger equation:

$$\begin{cases} \left(\nabla_t^2 + k^2\right)\psi(\boldsymbol{r}) = 0, & \boldsymbol{r} \in B \subseteq \mathbb{R}^2, \\ \psi(\boldsymbol{r}) = 0, & \boldsymbol{r} \in \partial B, \end{cases} \tag{1}$$

where ψ is the quantum mechanics wave function of a point particle with mass m and energy U in a hard wall; B and ∂B denote the billiard domain and its boundary, respectively; and $k = \sqrt{2mU}/\hbar$ is the wavenumber (with $\hbar$ denoting the Plank constant). The formal analogy between the boundary-value problem in Equation (1) and the Helmholtz boundary-value problem – describing the transverse field distribution of the time-harmonic longitudinal electric field component in transverse-magnetic (TM) modes in a perfectly conducting waveguide with cross section B and boundary ∂B – is readily recognized. In the EM case, $k = 2\pi/\lambda$, with λ denoting the wavelength. Thus, corresponding results pertaining to ray-chaotic footprints in quantum physics apply to EM waves as well, with the "semi-classical" ($\hbar \to 0$) quantum regime corresponding to the high-frequency ($\lambda \to 0$) EM regime.

In what follows, we shall review some of the basic tools and available results. Although emphasis will be placed on the two-dimensional steady-state case (with implied $\exp(-i\omega t)$ time dependence), the *pulsed* regime will also be given attention in Section 4.3.3.

4.2 Nuts and Bolts

The eigenfunctions of the Helmholtz boundary-value problem in Equation (1) form a (countable) complete set [22],

$$\delta(\boldsymbol{r} - \boldsymbol{r}') = \sum_n \phi_n(\boldsymbol{r})\phi_n^*(\boldsymbol{r}'), \tag{2}$$

which leads to the eigenexpansion for the Green's function of Equation (1) as [22]

$$G(\boldsymbol{r}_a, \boldsymbol{r}_b; k) = \sum_n \frac{\phi_n(\boldsymbol{r}_a)\phi_n^*(\boldsymbol{r}_b)}{k^2 - k_n^2}. \tag{3}$$

Here, $\phi_n(\boldsymbol{r})$ are the eigenfunctions corresponding to the eigenvalues k_n. As is well known, in two-dimensional domains where the Helmholtz equation is coordinate-separable (and, hence, *a fortiori*, integrable), the index n in Equations (2) and (3) denotes non-negative integers that tag the number of eigenfunction *nodes* along the coordinate directions [22]. *No* systematic procedure is known for computing eigenfunctions and eigenvalues in ray-chaotically-inclined (and *a fortiori* non-separable) geometries. In this connection, *ray* representations can offer approximate alternatives. In the limit $k|\boldsymbol{r}_a - \boldsymbol{r}_b| \gg 1$, the Green's function in Equation (3) can be approximated as a sum of Geometrical Optics (GO) ray-field contributions (see, e.g., [6, 23])

$$G(\boldsymbol{r}_a, \boldsymbol{r}_b; k) \sim \sum_\nu \frac{D_\nu^{(a,b)}}{\sqrt{\ell_\nu^{(a,b)}}} \exp\left[i\left(k\ell_\nu^{(a,b)} - m_\nu \frac{\pi}{2} - \frac{\pi}{4} \right) \right]. \tag{4}$$

In Equation (4), the summation index ν runs over *all* multiply-reflected *rays* (the so-called *eigenrays*) connecting $\boldsymbol{r}_a$ and $\boldsymbol{r}_b$. For each ray in the sum, $\ell_\nu^{(a,b)}$ denotes the path length, and $m_\nu = 2n_\nu + c_\nu$ is the so-called Maslov index, with n_ν and c_ν denoting the number of boundary reflections and passages through caustics (with corresponding phase shifts), respectively. Moreover, the Jacobian determinant (divergence factor) $D_\nu^{(a,b)}$ accounts for the spreading (or convergence) of nearby rays (ray tube) [6, 23].

The Geometrical Optics representation in Equation (4) can be used in principle to evaluate the Green's functions in *general* (non-separable, and even ray-chaotic) domains, with second-order asymptotic accuracy [24]. Note that for chaotic ray trajectories, the divergence factor, $D_\nu^{(a,b)}$, is expected to decrease *exponentially* (on average) with distance along the ray.

The (global) *modal* and *ray* representations for the Green's function in Equations (3) and (4), respectively, constitute the simplest high-frequency asymptotic alternatives. Their connection is explored next.

4.2.1 Theoretical Foundations

The intimate connections between the modal and ray representations can be established systematically by recourse to the Poisson transformation [25],

$$\sum_p f(p) = \sum_q F(q), \tag{5}$$

where f and F are related through a Fourier transform,

$$F(q) = \int_{-\infty}^{\infty} f(\tau)\exp(iq\tau)d\tau. \tag{6}$$

Through Equation (5), a set of wave functions, f, sampled at (integer) modal indexes, p, is mapped into a set of wave functions, F, sampled at (integer) spectral indexes, q. In view of the duality properties of the Fourier transform, the originally *global* modal wave functions, f, are transformed into the wave objects, F (local plane waves or rays). Since neither the modal nor the ray representation is convenient for *all* source-observer locations, efforts have been made to combine these two complementary methodologies in a manner that seeks to exploit the best features of each. The outcome has been a comprehensive, rigorously based, self-consistent, *hybrid ray-mode algorithm*. This has clarified the ray-mode interplay through a series of spectral studies and wide-ranging applications to complex waveguiding environments (see [26] for a review). Extension of this methodology to *ray-chaotic* scenarios, though possible in principle, is not straightforward, mainly due to the lack of constructive analytic procedures for computing eigenvalues and eigenfunctions in such geometries. In this connection, useful tools could possibly be provided by windowed transforms, which highlight *local* spectral features of wave fields (see [27] and the references therein).

A fundamental connection between ray and modal spectral properties is established by the so-called "trace formulas" [24, 28], which allow one to extract information about the modal spectrum from complete enumeration of the closed (periodic) ray trajectories. We shall only allude to their derivation, referring the reader to [3, 6, 24] for details. Trace formulas are obtained by integrating the Green's function in Equation (3) over the billiard domain. In this connection, the spectral pole singularities in Equation (3) are handled as follows [22]:

$$\frac{1}{k^2-k_n^2} \to \lim_{\varepsilon\to 0^+} \frac{1}{\left(k^2+i\varepsilon\right)-k_n^2} = P\left(\frac{1}{k^2-k_n^2}\right) - i\pi\delta\left(k^2-k_n^2\right), \tag{7}$$

where P indicates the principal part. Integrating Equation (3) over the billiard domain, with $r_a = r_b$, and using Equation (7) as well as the eigenfunction normalization condition, one obtains

$$\mathrm{Im}\left[\iint_B G(r_a, r_a, k)\,dr_a\right] \sim -\pi\sum_n \delta\left(k^2-k_n^2\right). \tag{8}$$

for the imaginary part.

Equation (8) provides a *direct* and *rigorous* relation between the eigenvalue spectrum and the integral of the Green's function. In the high-frequency asymptotic limit, the Geometrical Optics expansion in Equation (4) can be used in Equation (8), thereby yielding

$$\mathrm{Im}\left[\iint_B \sum_\nu \frac{D_\nu^{(a,a)}}{\sqrt{\ell_\nu^{(a,a)}}} \exp\left[i\left(k\ell_\nu^{(a,a)} - m_\nu\frac{\pi}{2} - \frac{\pi}{4}\right)\right] dr_a\right] \sim -\pi\sum_n \delta\left(k^2-k_n^2\right). \tag{9}$$

Note that in the high-frequency limit, the factor $\exp\left(ik\ell_\nu^{(a,a)}\right)$ in the integrand on the left-hand side of Equation (9) oscillates very rapidly. One can therefore use the stationary-phase approximation to evaluate the corresponding integral. It can be verified that the stationary-phase condition,

$$\nabla\ell_\nu^{(a,a)} = 0, \tag{10}$$

selects the *closed periodic trajectories* [3, 6, 24], thereby reducing the integral in Equation (9) to a *sum* over all closed periodic trajectories. This remarkable result, known as the Gutzwiller "trace formula," provides a useful and intriguing (approximate) connection between modal spectra and closed periodic ray trajectories (in quantum physics, the integral on the left-hand side of Equation (8) is referred to as "trace"). The asymptotic evaluation of the integral in Equation (9) is technically rather involved. The reader is referred to [6], where the cases of regular and ray-chaotic systems are worked out in detail. The trace formula has been the key for theoretical and numerical investigations on the eigenspectrum statistics (see Section 4.3.1).

4.2.2 Numerical and Experimental Validation Tools

The theoretical foundations of "wave chaology" have strong *numerical* and *experimental* support, based on a set of *conjectures* backed by substantial numerical and experimental evidence. Several algorithms are available for numerical calculation of the eigenvalues and eigenfunctions of the Helmholtz equation in arbitrarily-shaped domains. In principle, the entire arsenal of numerical tools for modal analysis developed in microwave engineering can be utilized. However, the inherent interest in very-high-order modes (sometimes up the 10^5th order), and therefore in spectral ranges considerably wider than those in typical microwave applications, requires careful (and often problem-matched) numerical implementations. Use of finite-difference/element methods is typically unaffordable, and attention has been focused on two approaches. The first approach is the Boundary Integral Method [29], where wave functions are represented by dipole source distributions on the boundary (spatial-Kirchhoff parameterization). This technique is reliable and versatile, and has been applied successfully to a variety of billiard shapes. The second approach, based on plane-wave spectral decompositions [30, 31], is simpler and computationally more efficient, mainly due to use of simpler basis functions. In both approaches, the goal is to compute the unknown expansion coefficients by enforcing the boundary conditions and solving the resulting matrix problem.

On the experimental side, superconducting microwave cavities with high quality factors ($Q \approx 10^5 - 10^7$) and adequately narrow spectral lines have been used for laboratory testing of the eigenvalue and eigenfunction properties of regular and chaotic billiard resonators. Two-dimensional models have been implemented using "pillbox" shapes [32]. Good agreement between theory, numerical simulations, and measurements in two-dimensional and

three-dimensional experiments has usually been observed for eigenvalue statistics [32, 33], and for eigenfunction morphology and spatial statistics [34-36] (see also Sections 4.3.1 and 4.3.2, and the Web site maintained by S. Sridhar at Northeastern University [37]). More recently, optical measurements have been performed in connection with ray-chaotic multimode fibers (D-shaped cut-circle, as in Figure 1e) [38].

4.3 Main Results

In what follows, we shall compare and contrast the eigenvalue and eigenfunction properties of the solutions of the Helmholtz boundary-value problem in Equation (1) in *regular* and *ray-chaotic* billiard enclosures.

4.3.1 Eigenvalues

As is well known, the two-dimensional Helmholtz boundary-value problem in Equation (1) gives rise to a countably infinite discrete eigenspectrum. We shall label the eigenvalues with a single subscript, n, in ascending order with respect to their numerical value, so that $k_n^2 \le k_{n+1}^2$.

We first consider the "cumulative density function" (CDF), $N\left(k^2\right)$, of the eigenspectrum, which yields the number of eigenvalues k_n^2 such that $k_n^2 < k^2$. In view of the inherently *discrete* character of the eigenspectrum of Equation (1), the CDF $N\left(k^2\right)$ exhibits a *staircase* behavior. The asymptotic (high-frequency) form of its *smoothed* version, $\bar{N}\left(k^2\right)$, is accurately predicted by the formula

$$\bar{N}\left(k^2\right) \sim \frac{A_B k^2 - L_{\partial B} k}{4\pi}, \tag{11}$$

which was obtained by Balian and Bloch, extending previous results by Weyl [3]. In Equation (11), A_B and $L_{\partial B}$ denote the area and the perimeter of the domain B, respectively. Note that Equation (11) depends only on gross features, and is the same irrespective of whether the geometry is regular or ray-chaotic. The regular or ray-chaotic features of the enclosure are actually embedded within the *local fluctuations* over the smoothing scale [3, 6]. A clean way to highlight these features is via the neighboring-eigenvalue spacing, $S_n = k_{n+1}^2 - k_n^2$. Moreover, in order to minimize dependence on the specific geometry, it is expedient to consider a suitably normalized version of S_n [3, 6],

$$s_n \equiv \bar{N}\left(k_{n+1}^2\right) - \bar{N}\left(k_n^2\right), \tag{12}$$

where $\bar{N}\left(k^2\right)$ is given by the estimate in Equation (11). Looking at the ensemble statistical properties of the normalized neighboring spacing s_n in Equation (12), the following distinct features are observed:

- In *regular* billiards (e.g., the rectangle), the spacing statistics follow a Poisson probability density function (PDF) [39]:

$$w(s) = \exp(-s). \tag{13}$$

The *universal* validity of Equation (13) has been demonstrated theoretically by Berry and Tabor [39].

- In *completely ray-chaotic* billiards, the spacing statistics turn out to be accurately modeled by the Wigner-Rayleigh probability density function [40]:

$$w(s) = \frac{\pi}{2} s \exp\left(-\frac{\pi s^2}{4}\right). \tag{14}$$

Strong theoretical [41], numerical [32, 42, 43], and experimental [32, 33] support of this conjecture can be found in the literature.

Note that the above-summarized properties are *universal*, i.e., *independent* of the *particular* chosen geometry. Deviations from the universal distribution in Equation (14) have been observed for ray-chaotic billiards that also admit (marginally-stable) closed ray trajectories (e.g., the stadium in Figure 1d) [32, 33]. However, the general problem concerning the eigenvalue spacing statistics of systems where regular and chaotic dynamics coexist is rather complicated and as yet unsettled (see [44]).

Figure 7 displays the Poisson and Wigner-Rayleigh probability density functions in Equations (13) and (14), respectively. It is observed that in regular billiards, the probability density function is peaked at $s = 0$ (i.e., zero spacing) and exhibits a long tail, thus favoring *modal degeneracy* and *poorly-correlated random-like clustering*. Conversely, in ray-chaotic billiards, the probability density function is peaked around a certain (nonzero) spacing

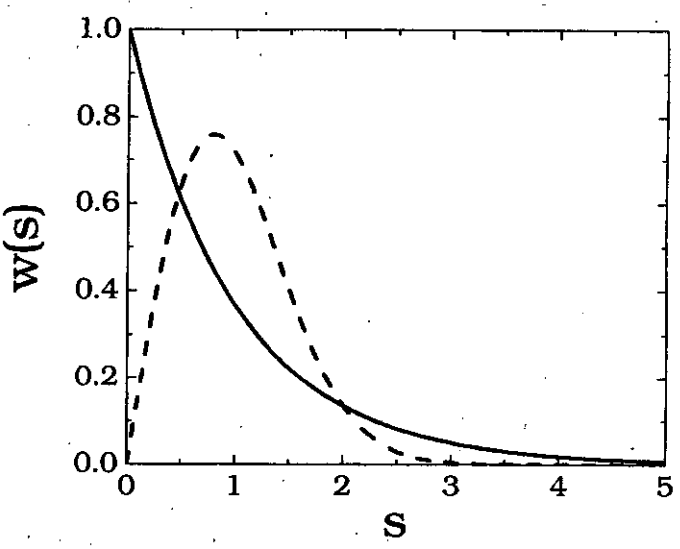

Figure 7. The probability density functions (PDF) of neighboring-eigenvalue spacing for regular and ray-chaotic enclosures. The solid red line is the Poisson PDF in Equation (13) (regular). The dashed blue line is the Wigner-Rayleigh PDF in Equation (14) (ray-chaotic).

value, thus rendering modal degeneracy unlikely, and favoring a more regular spacing. One is therefore led to the puzzling conclusion that eigenvalues in *regular* geometries turn out to be *randomly distributed*, whereas in *ray-chaotic* geometries they are *more correlated*. Incidentally, this striking oddity (the "hidden harmony" recalled by Heraclitus' quote at the beginning of the paper) is one of the main reasons why many scientists became interested in the subject.

Remarkably, the Wigner-Rayleigh distribution is intimately tied to the spectral (eigenvalue) ensemble statistics of real, symmetric, $N \times N$ *random matrices* [45], the elements a_{ij} of which are zero-mean Gaussian-random numbers with variance $\sigma_{ij} = \sqrt{\left(1+\delta_{ij}\right)N^{-1}}$ (Gaussian orthogonal ensemble). In particular, it can be shown that the probability density function in Equation (14) *exactly* describes the 2×2 matrix case; however, it also yields accurate estimations for the case of large matrices $\left(N \to \infty\right)$, which applies here [45]. The spectral statistics of ray-chaotic systems without time-reversal symmetry (e.g., nonreciprocal media) are described by a different (Gaussian unitary) ensemble of complex Hermitian random matrices [3, 6, 40].

Random matrices were introduced by Wigner [46] and Dyson [47] to describe the spectra of *complex* quantum systems (e.g., atomic nuclei), the Hamiltonians of which are not known in detail. During the last decades, they have emerged as a powerful and versatile tool in a variety of problems in pure and applied science. We merely mention the recently established connection between random matrices (and thus, indirectly, wave chaology) and the celebrated Riemann Hypothesis in number theory [48], and their practical application in wireless communication as effective statistical models of complex array-antenna-based channels [49].

4.3.2 Eigenfunctions

The (high-frequency) asymptotic properties of the eigenfunctions in regular or ray-chaotic geometries can be understood heuristically by noting that [50]

- In *regular* billiards (e.g., the rectangle), the wave field at each point results from the superposition of plane waves (rays) from *a finite number* of possible directions.
- In *completely ray-chaotic* billiards, the wave field is expected to be a superposition of a multitude of plane waves, with *fixed* wave vector amplitude, and *uniform* direction and phase distribution [50].

The random-plane-wave (RPW) conjecture, whereby the *ergodic* property of the ray trajectories is inherited by the eigenfunctions, was formulated by Berry [50] and Voros [51], capitalizing on previous work by Shnirelman [52]. This model yields very general characterizations of the eigenfunction spatial statistics. Specifically, the eigenfunction spatial samples form a zero-average Gaussian ensemble, with spatial field correlation exhibiting peculiar (universal) forms [50]. For the two-dimensional case, one obtains [50]

$$C(\boldsymbol{r}) \equiv \frac{\left\langle \phi_n\left(\boldsymbol{r}+\frac{\boldsymbol{r}'}{2}\right)\phi_n^*\left(\boldsymbol{r}-\frac{\boldsymbol{r}'}{2}\right)\right\rangle_{\boldsymbol{r}'}}{\left\langle \left|\phi_n\right|^2\right\rangle_{\boldsymbol{r}'}} \sim J_0\left(k_n|\boldsymbol{r}|\right), \qquad (15)$$

where J_0 denotes the zeroth-order Bessel function of the first kind [51]. Moreover, $\langle\ \rangle_{\boldsymbol{r}'}$ denotes a spatial average (with respect to $\boldsymbol{r}'$) over an interval centered at $\boldsymbol{r}$ and spanning several wavelengths [50].

The random-plane-wave (RPW) model has been shown to capture the essential statistical properties (both numerically predicted [38, 43] and measured [35]) of high-frequency *ergodic* wave functions in ray-chaotic billiards. It may be noted that similar random-plane-wave models have been utilized successfully to characterize complex radar signatures [12], as well as (narrowband) EM reverberating enclosures [54].

The remarkable connection with random matrices, already noted for the eigenvalues, has been found to also hold for the eigenfunctions [55]. Indeed, the probability density function of the eigenvector components of Gaussian-random matrices, like those introduced in Section 4.3.1, turns out to be [43, 45]

$$w(\phi_n) \propto \frac{\Gamma\left(\frac{N}{2}\right)}{\pi^{1/2}\Gamma\left(\frac{N-1}{2}\right)}\left(1-\phi_n^2\right)^{\frac{N-3}{2}}$$

$$\underline{N \to \infty} \quad \left(\frac{N}{2\pi}\right)^{1/2} \exp\left(-\frac{N\phi_n^2}{2}\right), \qquad (16)$$

where Γ denotes the Gamma function [53]. It can be verified that the two expressions in Equation (16) are already hardly distinguishable at $N \sim 100$. Again, deviations from these universal behaviors have been observed in ray-chaotic billiards that exhibit non-isolated marginally-stable periodic ray trajectories (see, e.g., [36]).

A typical high-frequency ergodic eigenfunction of the stadium billiard (from [30]) is shown in Figure 8a. A complicated random-like field pattern, well described statistically by the random-plane-wave model, is observed. An example of a *regular* quasi-plane-wave eigenfunction, tied to the non-isolated marginally-stable ray trajectory for vertical bouncing between the straight wall sections, is displayed in Figure 8b. Such behavior represents an example of the above-mentioned deviations from universality. For the stadium geometry, as for all ray-chaotic geometries that admit (albeit unstable) closed ray-trajectories, a further remarkable phenomenon is observed: certain *irregular* high-frequency eigenfunctions exhibit narrow regions of enhanced intensity along one or several *closed unstable* ray-paths (see, e.g., Figure 8c). These anomalous localization phenomena (named "scars") were first predicted numerically by Heller [30], and observed subsequently by Sridhar [34] in a microwave pillbox resonator experiment, using a "cavity perturbation" technique. Note that the presence of intensity ridges in the wave-field pattern is not necessarily in contrast with the random-plane-wave assumption. In [56], for example, numerical simulations were presented that revealed that large ($\sim 10^4$) random-wave superpositions might develop random networks of intensity-enhanced ridges (termed "scarlets") on scales $\sim 10-100\lambda$. However, what is really striking about scars is the anomalous interplay between *ray* and *wave* dynamics, whereby ray trajectories that are *unstable* (and thus hard to observe in a ray picture) show up very clearly in the *wave* dynamics, having been *stabilized* via constructive interference. We shall not be concerned here with the underlying theory; the interested reader is referred to [57] for further details.

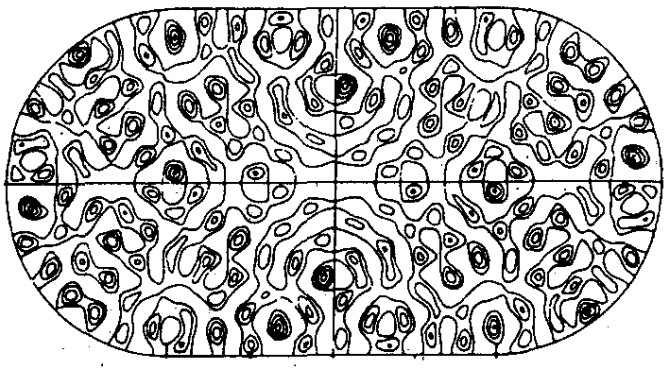

Figure 8a. A contour plot of a typical high-order ergodic eigenfunction in the stadium enclosure (from [30], with permission). The dark regions have the highest intensity.

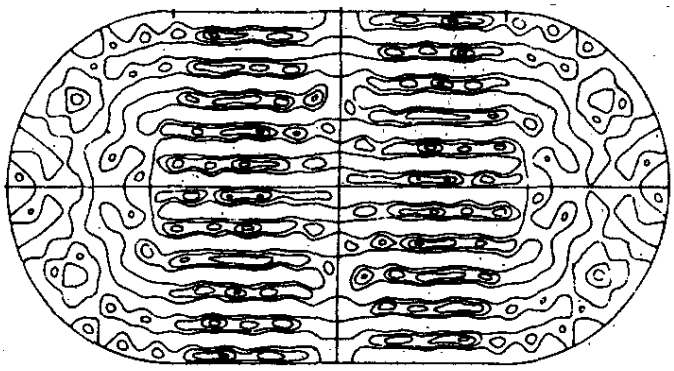

Figure 8b. A contour plot of a typical high-order regular quasi-plane-wave eigenfunction related to the non-isolated marginally-stable ray trajectory bouncing vertically between the straight walls in the stadium enclosure (from [30], with permission). The dark regions have the highest intensity.

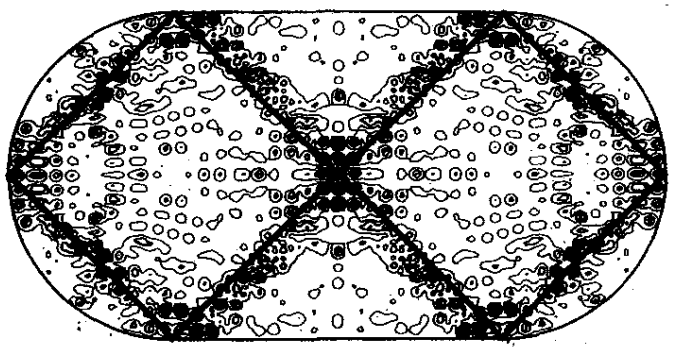

Figure 8c. A contour plot of a typical high-order eigenfunction featuring anomalous field localization ("scar") in the vicinity of an unstable periodic trajectory (shown solid) in the stadium enclosure (from [30], with permission). The dark regions have the highest intensity.

Additional distinct features of high-frequency eigenfunctions in ray-chaotic enclosures are related to the *erratic, self-avoiding* appearance of the nodal lines (zero levels). Although this feature appears in *regular* geometries as well, and is indeed a *generic* property of Helmholtz boundary-value problems [58], recent studies have evidenced significant differences in the eigenfunction nodal-domain statistics for regular and ray-chaotic geometries [59].

4.3.3 Pulsed Problems

The complete analogy between quantum physics and EM, so far exploited for time-harmonic excitation, breaks down in the presence of *pulsed* excitation, whereby the equivalence between the wave equation and the time-dependent Schrödinger equation holds only in particular approximated (e.g., paraxial) regimes. Therefore, known results from quantum physics concerning possible ray-chaotic footprints in the pulsed wave dynamics (see, e.g., [31, 60]) are not directly applicable to the EM counterpart. In this connection, some original numerical EM results will be presented and discussed in Section 5.

However, interesting results have recently been obtained in acoustic applications of ray-chaos-enhanced time-reversal focusing [61], for which the EM analogy is rather straightforward. In typical time-reversal focusing applications, a wave field generated, for example, by a point source is space-time sampled over a suitably large observation domain. Exploiting the time-symmetry of the wave equation, this signal is *re-focused back* to the source region via re-injecting the time-reversed versions of the sampled waveforms. The focusing resolution is clearly limited by the (finite) extent of the sampling domain, but the use of reflecting walls and/or random scatterers has been suggested to achieve (via multipath) a larger *synthetic aperture*, while keeping limited-size transmitter/receiver arrays [61]. From this perspective, the *ergodic* (in the terminology of Appendix B) properties of ray-chaotic enclosures – whereby the time history at *any* observation point in the enclosure contains information about the *entire* phase space – offer the suggestive possibility of trading *spatial* sampling with *temporal* sampling. Under these conditions, one could think of achieving time-reversal focusing using *only one* transmitter/receiver. This possibility has been demonstrated theoretically and experimentally in a series of papers by Fink and co-workers (see [62] and the references therein). As observed in [62], this represents an instructive and counter-intuitive paradigm, where chaotic/disordered multipath is exploited to *enhance* the amount of *coherently* transmitted information, which might lead to potential improvements in wireless technology.

5. Numerical Example: Pulsed Wave-Packet Propagation

As already noted in Section 4.3.3, the lack of a perfect analogy between the *wave* equation and the time-dependent Schrödinger equation prevents direct application of wave chaology results available from quantum physics to *pulsed* EM wave-packet dynamics. Here, we present a preliminary full-wave investigation of short-pulse EM wave-packet propagation in ray-chaotic enclosures, using a numerical approach based on the Finite-Difference Time-Domain (FDTD) Method [63]. The configuration of interest is the stadium billiard in Figure 1d, where, to minimize the computational effort, we exploited spatial symmetry, thereby restricting our attention to a single quadrant (Figure 9a); the simulation parameters are listed in the figure caption. A TM-polarized two-dimensional wave packet, with y-directed electric field E_y, was injected into the enclosure via a "hard-source" [63], i.e., enforcing the field distribution on an equivalent aperture at $z = z_A$,

$$E_y(x, z_A, t) = g(x - x_A)\, p\left[t - c^{-1}(x - x_A)\sin\theta_A\right], \quad (17)$$

where c is the wave speed; $g(x)$ is a cosine tapering (see Fig-

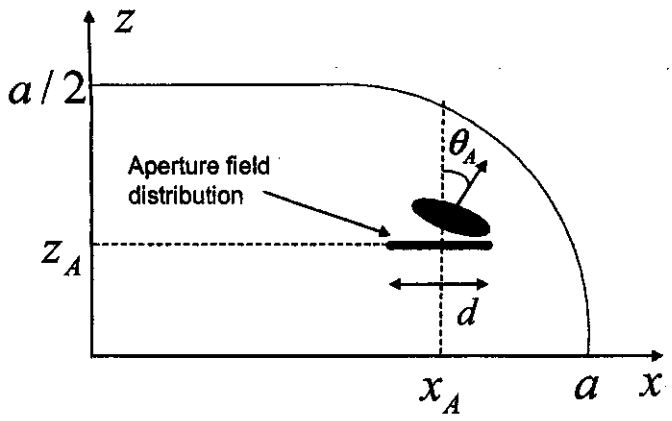

Figure 9a. The geometry and parameters pertaining to the Finite-Difference Time-Domain (FDTD) simulations in Section 5, for a quarter-stadium enclosure and a "hard-source" aperture field distribution for (TM-polarized) wave packet launching $a=2$, $d=0.5$, $x_A=1.5$, $z_A=0.25$, $\theta_A=30°$). The FDTD cell was $\Delta_x=\Delta_z=0.01cT$ (corresponding to 20 points per minimum wavelength).

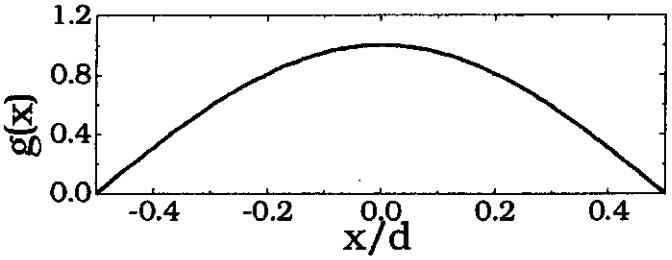

Figure 9b. As in Figure 9a, but for a cosine spatial aperture tapering.

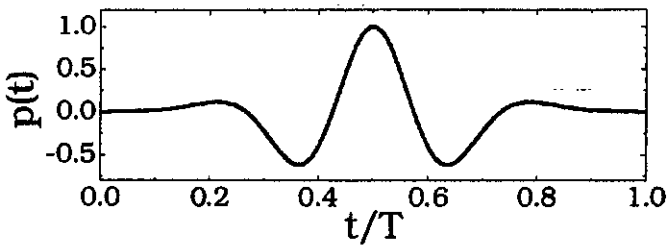

Figure 9c. As in Figure 9a, but for a fourth-order Rayleigh pulse $(cT=a/20)$.

ure 9b); and $p(t)$ is a fourth-order Rayleigh pulse of length T (Figure 9c), assumed to be *short* with respect to the enclosure size a ($cT=a/20$). Moreover, θ_A and x_A were used to steer the wave packet and to adjust the launch position. The wave packet's evolution was tracked using a standard FDTD algorithm [63], with spatial discretization $\Delta_x=\Delta_z=0.01cT$ (corresponding to 20 samples per minimum wavelength).

A typical evolution is shown in Figure 10, via instantaneous snapshots of the wave field distribution at various times. While bouncing around the walls, along the ray-path skeleton, the wave packet underwent focusing at the concave curved wall and natural spreading elsewhere (including straight-wall reflection), progressively losing its initial space-time localization. At time $t=1000T$ (see Figure 10d), corresponding on average to about 20 roundtrips in the enclosure, the wave packet had already uniformly covered the entire enclosure. The initially localized energy was spread across the mode spectrum, and it was not surprising to observe that the field distribution resembled that of an *ergodic* eigenfunction (see Figure 8a). In his quantum-physics investigation, Heller [31] observed a qualitatively similar behavior. He quoted the picturesque description used by E. M. Forster in *A Passage to India* [64] to portray the "Marabar caves" (examples of ray-chaotic enclosures in nature):

> The echo in a Marabar cave...is entirely devoid of distinction....Hope, politeness, the blowing of a nose, the squeak of a boot, all produce "boum."

Statistical analysis of the late-time spatial field distributions led us to results similar to those in Section 4.3.2. In particular, reasonably good agreement with the Gaussian prediction for the late-time field probability density function (PDF) was found uniformly across the enclosure, as exemplified in Figure 11. Similar results were observed for a broad range of wave packet initial conditions, with the anticipated exceptions of those leading to prolonged vertical bouncing between the straight wall portions. The above statistics and those that follow were computed over square observation domains with size $1.25cT$ (sufficiently large so as to yield meaningful statistics, and yet sufficiently small so as to reveal possible spatial variations). Figure 12 shows samples of the late-time field spatial correlation,

$$C(x_0,z_0,t)=\frac{\iint_D E_y\left(x+\frac{x_0}{2},z+\frac{z_0}{2},t\right)E_y\left(x-\frac{x_0}{2},z-\frac{z_0}{2},t\right)dxdz}{\iint_D E_y^2(x,z,t)dxdz}, \tag{18}$$

over different observation domains across the enclosure. The correlation turned out to be nicely *uniform* and *isotropic*, with a correlation length on the order of the pulse length, cT. Again, similar results were observed almost independently of the wave-packet initial conditions, and seemed to be consistent with those from random-wave models encountered in the time-harmonic case (see Section 4.3.2). We are currently working on extending the corresponding implications (e.g., Equation (15)) to the pulsed regime.

To sum up, these preliminary simulations seemed to indicate a late-time trend toward a *random-like ergodic* field distribution[1], with nicely uniform and robust (with respect to initial conditions) Gaussian statistical properties. Such characteristics, anticipated in [19] via qualitative ray analysis, could be of potential interest for wideband EM compatibility/interference test beds (see Section 2.3). We have also performed the same statistical analysis for *regular* (e.g., rectangular and circular) geometries. Preliminary results (not shown for brevity) seem to suggest more *regular* field distributions (even at late times), with significant deviations from Gaussian statistics and isotropic spatial correlation, and increased sensitivity to wave-packet initial conditions.

[1] Due to the limited temporal extent of our numerical simulations, we cannot rule out the possible presence of cyclic re-localization phenomena similar, e.g., to the Fermi-Pasta-Ulam recurrence observed in weakly-nonlinearly-coupled arrays of oscillators [65].

6. Conclusions and Perspectives: What We Can Learn from Playing Chaotic Billiards

A compact review of results on time-harmonic wave propagation in ray-chaotic scenarios has been attempted here. Discussion has been restricted to two-dimensional *internal* problems with perfectly conducting boundaries. New full-wave simulation results have also been presented to illustrate the evolution of a *pulsed* wave packet. The summary here is far from exhaustive, and some of the relevant issues involved are *as yet unsettled* (see [66], dealing with presumed exceptions to the generic regular/ray-chaotic features mentioned in Section 4). Concerning problem complexity, it is suggestive to use a three-tiered classification of EM wave environments. The least complex scenario applies when the Helmholtz equation is *coordinate-separable*. Waves in such systems are obtained by solving suitable one-dimensional ordinary differential equations, which can be integrated analytically: *no* ray-chaos or wave irregularity evolves, the ray/mode machinery works without pain, and the eigenvalues are simply obtained from the separation constants. Most complex are configurations that exhibit *strong ray chaos*. To date, there is *no* simple recipe for solving the related EM boundary-value problem (BVP), *nor* to compute eigenvalues/eigenfunctions in a general, systematic fashion. In between stay scenarios that are *globally non*-separable, but possibly *locally* or *weakly* separable, and/or are still characterized by *regular* ray dynamics ("integrable," in the terminology of Appendix B). Traditional EM analytic modeling has largely dealt with such configurations, developing tools such as the Geometrical Theory of Diffraction [67], ray-mode algorithms [26], adiabatic approximations [68], network architectures [69], etc., pertaining to a variety of fairly "regular" real-world problems. For EM wave interactions with more *complex/irregular* propagation environments, exemplified by urban or rural conglomerates, photonic waveguides with random defects, etc., the inherent irregular (non-separable) and/or disordered geometries may have a tendency toward ray chaos, resulting in field evolutions that eventually exhibit extreme sensitivity to changes in source or observation position, frequency, etc. In most of these circumstances, *statistical* descriptions would be appropriate [70].

The ray-chaotic "billiards" discussed in this paper are scenarios with *deceptively simple* geometric/constitutive features, which however exhibit *fairly complex* EM responses. We note that certain tools and models originally developed and applied in close connection with wave chaology, such as random-plane-wave models and random-matrix models, have found successful application in complex EM wave propagation scenarios, such as characterization of radar signatures [12], reverberating enclosures [54], and wireless channels [49]. Assembling a tool box of algorithms for complex-disordered system modeling in various wave-disciplines is likely to become increasingly relevant for wave-dynamical studies in this important problem area.

7. Appendix A

7.1 A Primer on Chaos

This appendix is intended for the reader with *no* previous knowledge on the subject. The discussion below may hopefully give some flavor of chaos concepts and tools.

Pedagogically, chaos is best introduced by running some paradigm cases on a computer. The main diagnostic tools should be more readily understandable thereafter. The following prototype chaotic systems share the status of paradigms, for historical/conceptual reasons [1-3]:

a) The logistic map:

$$x_{n+1} = \lambda x_n (1 - x_n). \tag{19}$$

b) The forced[2] Duffing oscillator (here and henceforth the overdot denotes time differentiation):

$$\ddot{x} = -kx - x^3 + A\cos\Omega t. \tag{20}$$

c) The Lorenz fluid-convection equations:

$$\begin{cases} \dot{x} = \sigma(y - x), \\ \dot{y} = rx - y - xz, \\ \dot{z} = -bz + xy. \end{cases} \tag{21}$$

d) The Bunimovich stadium billiard in Figure 1d, where a point particle moves without friction, bouncing elastically at the walls (see Section 3).

For suitable values of the initial conditions and system parameters, these systems may exhibit regular (predictable) solutions. However, for some values of the problem parameters (e.g., $\lambda \geq 3.5699$ in Equation (19); $k = 0.1$ and $9.8 \leq A \leq 13.4$ in Equation (20); $\sigma = 10$, $b = 8/3$, $r = 28$ in Equation (21)), the time histories of these systems may exhibit *no* evident regularity, and may look almost unpredictable, similar to broadband noise, despite the fact that neither stochastic parameters nor noisy forcing inputs are present. This is a loose description of chaos.

Chaos can be diagnosed by going through the following behavioral checklist:

i) Broadband frequency spectrum of the solutions (significant if only a few spectral lines should be expected).

ii) Trajectories either filling most of the phase space and/or the embedding delay space (loss-free systems), or clustering into *fractal* sets (lossy systems, strange attractors). We recall that, for continuous and discrete time systems with state variables x, the phase and embedding-delay spaces are defined as $(x, \dot{x})$ and (x_n, x_{n+N}), where N is a suitable integer.

iii) Strong sensitivity to slight changes in the initial conditions, i.e., fast loss of information about the initial state upon evolution, measured either in terms of Lyapounov exponents (exponential divergence rate of system evolutions from nearby initial conditions), or Sinai entropy (exponential divergence rate of uncertainty volume) [1-3].

[2] In this connection, we recall a theorem by Poincaré stating that chaos can only occur in free-running systems with no less than two degrees of freedom. Systems with one degree of freedom can be chaotic *only* in the *forced* case.

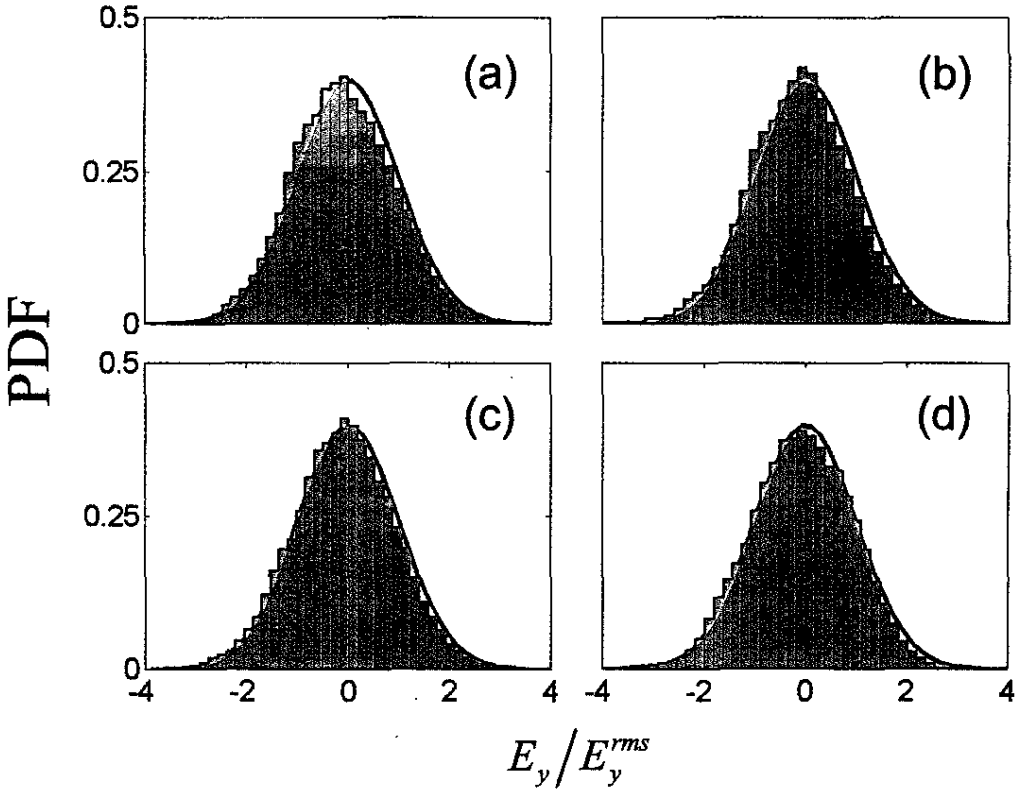

Figure 11. The late-time ($t = 1000T$) field probability density function (PDF) estimated over a square domain with size $1.25cT$ (1.5×10^4 samples) centered at various positions across the enclosure. The solid red curve is the Gaussian prediction. The bars are the numerical histogram. The geometry and parameters were as in Figure 9. (a) $(x,z) = (0.275, 0.275)$, (b) $(x,z) = (0.775, 0.525)$, (c) $(x,z) = (0.925, 0.175)$, (d) $(x,z) = (1.375, 0.725)$.

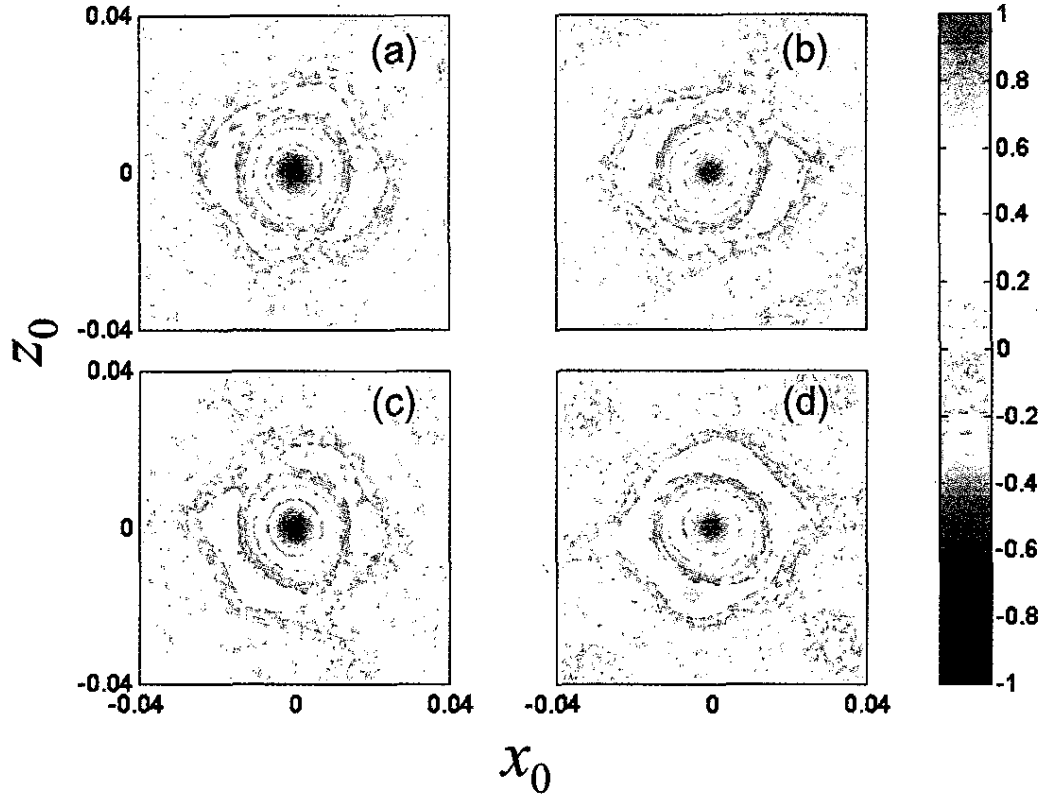

Figure 12. As in Figures 11a-11d, but showing the spatial field correlation in Equation (18).

Test iii) above can be shown to be the most conclusive. The Lyapounov exponents are computed by tracking the evolution of initial conditions from a *tiny* spherical hyper-volume in the phase space through the locally linearized dynamics of the system. As a result, a spherical hyper-volume of radius $\Delta x(0)$ will develop into a hyper-ellipsoidal volume with principal axes having lengths $\Delta x_i(t)$. The Lyapounov exponents, λ_i, can then be formally defined as

$$\lambda_i = \lim_{\substack{t\to\infty \\ \Delta x(0)\to 0}} \frac{1}{t}\log\frac{\Delta x_i(t)}{\Delta x(0)}. \qquad (22)$$

The reader is referred to [1-3] for theoretical and computational details.

8. Appendix B

8. Ranking Disorder: How Chaotic Is Chaos?

We borrow from [1, 3, 6] the following classification of dynamical systems in an order of increasing *irregularity*:

8.1 Integrable Systems

There are several (more or less restrictive) definitions of "integrable systems," usually tied to the analytic integrability of the relevant dynamical (ray) evolution, i.e., to the existence of suitable independent "constants of motion" (see [1, 3, 6] for details). Here, we merely emphasize that integrability implies *regular* (i.e., non-chaotic) ray dynamics. Coordinate-separable systems are *always* integrable (the separation constants being the required constants of motion). However, non-separability *does not* imply non-integrability. For example, some polygonal billiards are non-separable but still integrable. Note that non-integrability is only a *necessary*, but not a sufficient, condition for chaotic dynamics.

8.2 Ergodic Systems

Ergodic (stationary) systems share the following property: the average at (any) fixed time of any dynamical variable over *several realizations* (e.g., trajectories originating from different initial conditions) is the same as the average computed over *the time history* of a *single* realization.

8.3 Mixing Systems

The "mixing" property of a system (with respect to its dynamical evolution) has basically the same meaning that we use to describe the mixing of a drop of cream in a cup of coffee (see [3] for a rigorous technical definition).

8.4 K(olmogoroff)-systems

These systems are characterized by at least one positive Lyapounov exponent for *some* initial conditions. The chaotic billiards in Figures 1d-1f are simple examples of K-systems.

8.5 C-systems

These systems, like K-systems, have positive Lyapounov exponent(s), but for *arbitrary* initial conditions. In such systems, *no* closed (periodic) trajectories, albeit unstable, exist. A C-system example is given by the chaotic billiard in Figure 1g.

8.6 B(ernoulli)-systems

For these systems, the dynamics can be represented by suitable *symbolic dynamics* consisting of full (i.e., unrestricted) *shifts* over (generally bi-infinite) strings of symbols taken from a *finite* alphabet [3].

Chaotic systems are *always* ergodic, whereas ergodicity does *not* necessarily imply chaos. Chaotic systems are not necessarily mixing (see [3] for constructive examples). The simultaneous occurrence of chaos and mixing is occasionally called *hard chaos*.

9. Acknowledgements

The authors acknowledge several stimulating discussions with Prof. Giorgio Franceschetti ("Federico II" University of Naples, Italy, and UCLA, USA) and Prof. Paolo Luchini (University of Salerno, Italy). L. B. Felsen acknowledges partial support from Polytechnic University, Brooklyn, NY 11201 USA.

10. References

1. A. J. Lichtenberg and M. A. Liebermann, *Regular and Stochastic Motion*, New York, Springer, 1983.

2. L. O. Chua and S. Parker, "Chaos: A Tutorial for Engineers," *Proceedings of the IEEE*, **75**, 8, August 1987, pp. 982-1008.

3. E. Ott, *Chaos in Dynamical Systems*, Cambridge, Cambridge University Press, 1993.

4. *Proceedings of the IEEE*, "Special Issue on Chaotic Systems," **75**, 8, August 1987.

5. M. V. Berry, "Quantum Chaology," *Proceedings of the Royal Society of London*, **A413**, 1987, pp. 183-198.

6. M. C. Gutzwiller, *Chaos in Classical and Quantum Mechanics*, New York, Springer, 1991.

7. R. N. Madan (ed.), *Chua's Circuit: A Paradigm for Chaos*, World Scientific Series on Nonlinear Science, Series B, **1**, November 1993.

8. N. B. Abraham, E. Arimondo, and R. W. Boyd, "Instabilities, Dynamics and Chaos in Nonlinear Optical Systems," in N. B. Abraham, F. T. Arecchi, and L. A. Lugiato (eds.), *Instability and Chaos in Quantum Optics*, NATO-ASI B177, New York (NY), Plenum Press, 1988, pp. 375-391.

9. V. Pierro and I. M. Pinto, "Radiation Pressure Induced Chaos in Multipendular Fabry Perot Resonators," *Physics Letters A*, **185**, 1, January 1994, pp. 14-22.

10. L. M. Pecora and T. L. Carroll, "Synchronization in Chaotic Systems," *Physical Review Letters*, **64**, 8, February 1990, pp. 821-824.

11. X. Yang, T. X. Wu, and D. L. Jaggard, "Synchronization Recovery of Chaotic Wave Through an Imperfect Channel," *IEEE Antennas and Wireless Propagation Letters*, **1**, 8, 2002, pp. 154-156.

12. A. J. Mackay, "An Application of Chaos Theory to the High Frequency RCS Prediction of Engine Ducts," in P. D. Smith and S. R. Cloude (eds.), *Ultra-Wideband, Short-Pulse Electromagnetics 5*, New York (NY), Kluwer/Academic Publishers, 2002, pp. 723-730.

13. C. Gmachl, F. Capasso, E. E. Narimanov, J. U. Nöckel, A. D. Stone, J. Faist, D. L. Sivco, and A. Y. Cho, "High-Power Directional Emission from Microlasers with Chaotic Resonators," *Science*, **280**, 5369, June 1998, pp. 1556-1564.

14. http://darkwing.uoregon.edu/~noeckel/microlasers.html (Web page maintained by J. U. Nöckel at the University of Oregon).

15. P. Corona, J. Ladbury, and G. Latmiral, "Reverberation-Chamber Research – Then and Now: A Review of Early Work and Comparison with Current Understanding," *IEEE Transactions on Electromagnetic Compatibility*, **EMC-44**, 1, February 2002, pp. 87-94.

16. L. Cappetta, M. Feo, V. Fiumara, V. Pierro, and I. M. Pinto, "Electromagnetic Chaos in Mode Stirred Reverberation Enclosures," *IEEE Transactions on Electromagnetic Compatibility*, **EMC-40**, 3, August 1998, pp. 185-192.

17. J. G. Kostas and B. Boverie, "Statistical Model for a Mode-Stirred Chamber," *IEEE Transactions on Electromagnetic Compatibility*," **EMC-33**, 4, November 1991, pp. 366-370.

18. P. Corona, G. Latmiral, and E. Paolini, "Performance and Analysis of a Reverberating Enclosure with Variable Geometry," *IEEE Transactions on Electromagnetic Compatibility*," **EMC-22**, 1, 1980, pp. 2-5.

19. V. Fiumara, V. Galdi, V. Pierro, and I. M. Pinto, "From Mode-Stirred Enclosures to Electromagnetic Sinai Billiards: Chaotic Models of Reverberation Enclosures," *Proceedings of the 6th International Conference on Electromagnetics in Advanced Applications (ICEAA '99)*, Torino, Italy, September 15-17, 1999, pp. 357-360.

20. T. Kottos, U. Smilansky, J. Fortuny, and G. Nesti, "Chaotic Scattering of Microwaves," *Radio Science*, **34**, 4, July-August 1999, pp. 747-758.

21. G. Castaldi, V. Fiumara, V. Galdi, V. Pierro, I.M. Pinto, and L.B. Felsen, "Ray-Chaotic Footprints in Deterministic Wave Dynamics: A Test Model with Coupled Floquet-Type and Ducted-Type Mode Characteristics," *IEEE Transactions on Antennas and Propagation*, **AP-53**, 2, February 2005 (in print).

22. R. Courant and D. Hilbert, *Mathematical Methods of Theoretical Physics*, New York, Wiley, 1953.

23. L. B. Felsen and N. Marcuvitz, *Radiation and Scattering of Waves*, Englewood Cliffs, NJ, Prentice Hall, 1973; Piscataway, NJ, IEEE Press, 1994.

24. M. C. Gutzwiller, "Periodic Orbits and Classical Quantization Conditions," *Journal of Mathematical Physics*, **12**, 1971, pp. 343-358.

25. A. Papoulis, *Signal Analysis*, New York, McGraw-Hill, 1977.

26. L. B. Felsen, "Progressing and Oscillatory Waves for Hybrid Synthesis of Source Excited Propagation and Diffraction," *IEEE Transactions on Antennas and Propagation*, **AP-32**, 8, August 1984, pp. 775-796.

27. L. Carin and L. B. Felsen, "Wave-Oriented Data Processing for Frequency and Time Domain Scattering by Nonuniform Truncated Arrays," *IEEE Antennas and Propagation Magazine*, **36**, 3, June 1994, pp. 29-43.

28. R. Balian and C. Bloch, "Distribution of Eigenfrequencies for the Wave Equation in a Finite Domain: III. Eigenfrequency Density Oscillations," *Annals of Physics*, **69**, 1972, pp. 76-160.

29. R. J. Riddel, Jr., "Boundary-Distribution Solution of the Helmholtz Equation for a Region with Corners," *Journal of Computational Physics*, **31**, 1979, pp. 21-41.

30. E. J. Heller, "Bound-State Eigenfunctions of Classically chaotic Systems: Scars of Periodic Orbits," *Physical Review Letters*, **53**, 16, October 1984, pp. 1515-1518.

31. E. J. Heller, "Wavepacket Dynamics and Quantum Chaology," in M.-J. Giannoni, A. Voros, and J. Zinn-Justin (eds.), *Chaos and Quantum Physics*, New York, Elsevier, 1991, pp. 549-663.

32. H. Alt, C. Dembowski, H.-D. Gräf, R. Hofferbert, H. Rehfeld, A. Richter, and C. Schmit, "Experimental vs. Numerical Eigenvalues of a Bunimovich Stadium Billiard – A Comparison," *Physical Review E*, **60**, 3, September 1999, pp. 2851-2858.

33. A. Kudrolli and S. Sridhar, "Signatures of Chaos in Quantum Billiards: Microwave Experiments," *Physical Review E*, **49**, 1, January 1994, pp. R11-R14.

34. S. Sridhar, "Experimental Observation of Scarred Eigenfunctions of Chaotic Microwave Cavities," *Physical Review Letters*, **67**, 7, August 1991, pp. 785-788.

35. J. Stein and H-J. Stöckmann, "Experimental Determination of Billiard Wavefunctions," *Physical Review Letters*, **68**, 19, May 1992, pp. 2867-2870.

36. A. Kudrolli, V. Kidambi, and S. Sridhar, "Experimental Studies of Chaos and Localization in Quantum Wavefunctions," *Physical Review Letters*, **75**, 5, July 1995, p. 822-825.

37. http://sagar.physics.neu.edu (Web site maintained by S. Sridhar at Northeastern University).

38. V. Doya, O. Legrand, F. Mortessagne, and C. Miniatura, "Speckle Statistics in a Chaotic Multimode Fiber," *Physical Review E*, **65**, May 2002.

39. M. V. Berry and M. Tabor, "Level Clustering in the Regular Spectrum," *Proceedings of the Royal Society of London*, **356**, 1977, pp. 375-393.

40. M. V. Berry, "Classical Chaos and Quantum Eigenvalues," in S. Lundqvist, N. H. March, and M. P Tosi (eds.), *Order and Chaos in Nonlinear Physical Systems*, New York and London, Plenum Press, 1988, pp. 341-348.

41. P. Pechukas, "Distribution of Energy Eigenvalues in the Irregular Spectrum," *Physical Review Letters*, **51**, 11, September 1983, pp. 943-946.

42. O. Bohigas, M.-J. Giannoni, and C. Schmit, "Characterization of Chaotic Quantum Spectra and Universality of Level Fluctuation Laws," *Physical Review Letters*, **52**, 1, January 1984, pp. 1-4.

43. S. W. McDonald and A. N. Kaufman, "Wave Chaos in the Stadium: Statistical Properties of the Short-Wave Solution of the Helmholtz Equation," *Physical Review A*, **37**, 8, April 1988, pp. 3067-3086.

44. T. A. Brody, J. Flores, J. P. French, P. A. Mello, A. Pandey, and S. S. M. Wong, "Random Matrix Physics: Spectrum and Strength Fluctuations," *Review of Modern Physics*, **53**, 3, July 1981, pp. 385-479.

45. M. L. Mehta, *Random Matrices, Second Edition*, San Diego, Academic Press, CA, 1991.

46. E. P. Wigner, "Random Matrices in Physics," *SIAM Review*, **9**, 1967, p. 1-23.

47. F. Dyson, "Statistical Theory of the Energy Levels of Complex Systems, I., II., and III.," *Journal of Mathematical Physics*, **3**, 1962, p. 140-175.

48. M. V. Berry and J. P. Keating, "The Riemann Zeros and Eigenvalue Asymptotics," *SIAM Review*, **41**, 2, 1999, pp. 236-266.

49. A. L. Moustakas, H. U. Baranger, L. Balents, A. M. Sengupta, and S. H. Simon, "Communication Through a Diffusive Medium: Coherence and Capacity," *Science*, **287**, 5451, January 2000, pp. 287-290.

50. M. V. Berry, "Regular and Irregular Semiclassical Wavefunctions," *Journal of Physics A*, **10**, 12, December 1977, pp. 2083-2091.

51. G. Casati and J. Ford (eds.), *Stochastic Behavior in Classical and Quantum Hamiltonian Systems*, Lecture Notes in Physics, 93, Berlin, Springer-Verlag, 1979.

52. A. I. Shnirelman "Ergodic Properties of Eigenfunctions," *Uspekhi Matematicheskikh Nauk*, **29**, 6, 1974, pp. 181-182.

53. M. Abramowitz and I. E. Stegun, *Handbook of Mathematical Functions*, New York, NY, Dover, 1972.

54. D. A. Hill, "Plane-Wave Integral Representation for Fields in Reverberation Chambers," *IEEE Transactions on Electromagnetic Compatibility*, **EMC-40**, 3, August 1998, pp. 209-217.

55. F. M. Izrailev, "Chaotic Structures of Eigenfunctions in Systems with Maximal Quantum Chaos," *Physics Letters A*, **125**, 5, November 1987, pp. 250-252.

56. P. O'Connor, J. Gehlen, and E. J. Heller, "Properties of Random Superpositions of Plane Waves," *Physical Review Letters*, **58**, 13, March 1987, pp. 1296-1299.

57. M. V. Berry, "Quantum Scars of Classical Closed Orbits," *Proceedings of the Royal Society of London*, **243**, 1989, pp. 219-231.

58. K. Uhlenbeck, "Generic Properties of Eigenfunctions," *American Journal of Mathematics*, **98**, 1976, pp. 1059-1078.

59. G. Blum, S. Gnutzmann, and U. Smilansky, "Nodal Domain Statistics: A Criterion for Quantum Chaos," *Physical Review Letters*, **88**, March 2002, 114101.

60. A. Peres, "Stability of Quantum Motion in Chaotic and Regular Systems," *Physical Review A*, **30**, 4, October 1984, pp. 1610-1615.

61. M. Fink, "Time-Reversal Acoustics," *Physics Today*, **50**, 3, March 1997, pp. 34-40.

62. M. Fink and J. de Rosny, "Time-Reversed Acoustics in Random Media and in Chaotic Cavities," *Nonlinearity*, **15**, 1, January 2002, pp. R1-R18.

63. A. Taflove, *Computational Electrodynamics: The Finite-Difference Time-Domain Method*, Norwood, MA, Artech House, 1995

64. E. M. Forster, *A Passage to India*, London, Edward Arnold & Co., 1984.

65. E. Fermi, J. Pasta, and S. Ulam, *Collected Papers of Enrico Fermi*, Chicago, IL, University of Chicago Press, 1965.

66. P. Seba, "Wave Chaos in Singular Quantum Billiard," *Physical Review Letters*, **64**, 16, April 1990, pp. 1855-1858.

67. V. A. Borovikov and B. Ye. Kinber, *Geometrical Theory of Diffraction*, London, IEE Press, 1994.

68. L. B. Felsen and L. Sevgi, "Adiabatic and Intrinsic Modes for Wave Propagation in Guiding Environments with Longitudinal and Transverse Variation: Formulation and Canonical Test," *IEEE Transactions on Antennas and Propagation*, **AP-39**, 8, August 1991, pp. 1130-1136.

69. L. B. Felsen, M. Mongiardo, and P. Russer, "Electromagnetic Field Representations and Computations in Complex Structures I: Complexity Architecture and Generalized Network Formulation," *International Journal of Numerical Modeling: Electronic Networks, Devices and Fields*, **15**, 1, January-February 2002, pp. 93-107.

70. T. H. Lehman, "A Statistical Theory of Electromagnetics in Complex Cavities," *Interaction Notes*, **494**, Kirtland, NM, Phillips AFB Laboratories, 1993.

More References (Ordered by Subject)

Chaos Basics (Section 1)

J. Gleick, *Chaos*, New York, Viking Penguin Inc., 1987.

E. Lorenz, "Predictability: Does the Flap of a Butterfly's Wings in Brazil Set Off a Tornado in Texas?" paper originally delivered at the 139th meeting of the American Association for the Advancement of Science, Washington, DC, 1972; E. Lorenz, *The Essence of Chaos*, Seattle, University of Washington Press, 1993, Appendix I, pp. 181-184.

R. C. Hilborn, *Chaos and Nonlinear Dynamics: An Introduction for Scientists and Engineers, Second Edition*, Oxford, Oxford University Press, 2001.

A. L. Goldberger, "Nonlinear Dynamics, Fractals and Chaos: Applications to Cardiac Electrophysiology," *Annals of Biomedical Engineering*, **18**, 2, 1990, pp. 195-198.

R. M. A. Urbach, *Footprints of Chaos in the Markets: Analyzing Non-linear Time Series in Financial Markets and Other Real Systems*, London-New York, Financial Times Prentice Hall, 2000.

Ray-Chaotic Manifestations and Applications (Section 2.2)

K. B. Smith, M. G. Browm, and F. D. Tappert, "Ray Chaos in Underwater Acoustics," *Journal of the Acoustical Society of America*, **91**, 4, April 1992, pp. 1939-1949.

J. U. Nöckel, A. D. Stone, and R. K. Chang, "Q-Spoiling and Directionality in Deformed Ring Cavities," *Optics Letters*, **19**, 21, November 1994, pp. 1693-1695.

A. Mekis, J. U. Nöckel, G. Chen, A. D. Stone, and R. K. Chang, "Ray Chaos and Q-Spoiling in Lasing Droplets," *Physical Review Letters*, **75**, 14, October 1995, pp. 2682-2685.

T. Fukushima, S.A. Biellak, Y. Sun, and A.E. Siegman, "Beam Propagation Behavior in a Quasi-Stadium Laser Diode," *Optics Express*, **2**, 2, January 1998, pp. 21-28.

A. J. Mackay, "Application of Chaos Theory to Ray Tracing in Ducts," *IEE Proceedings on Radar, Sonar and Navigation*, **164**, 6, December 1999, pp. 298-304.

P. B. Wilkinson, T. M. Fromhold, R. P. Taylor, and A. P. Micolich, "Electromagnetic Wave Chaos in Gradient Refractive Index Optical Cavities," *Physical Review Letters*, **86**, 24, June 2001, pp. 5466-5469.

Ray-Chaotic Billiards (Section 3)

Ya. G. Sinai, "Dynamical Systems with Elastic Reflections," *Russian Mathematical Surveys*, **25**, 2, 1970, pp. 137-189.

L. A. Bunimovich, "Conditions of Stochasticity of Two-Dimensional Billiards," *Chaos*, **1**, 2, August 1991, pp. 187-193.

J. D. Meiss, "Regular Orbits for the Stadium Billiard," in P. Cvitanović, I. C. Percival, and A. Wirzba (eds.), *Quantum Chaos – Quantum Measurements*, Dordrecht, Kluwer Academic, 1992, pp. 145-166.

J. Wiersig, "Singular Continuous Spectra in a Pseudointegrable Billiard," *Physical Review E*, **62**, 1, July 2000, pp. R21-R24.

Wave Chaology (Section 4)

M. V. Berry, "Quantum Chaology, Not Quantum Chaos," *Physica Scripta*, **40**, 1989, pp. 335-336.

M. Tabor, *Chaos and Integrability in Nonlinear Dynamics*, New York, NY, John Wiley & Sons, 1989.

F. Haake, *Quantum Signatures of Chaos*, New York, NY, Springer, 1991.

Theoretical Tools and Results (Section 4.2.1)

M. V. Berry and J. P. Keating, "A Rule for Quantizing Chaos?," *Journal of Physics A*, **23**, 21, November 1990, pp. 4839-4849.

M. Sieber and F. Steiner, "Quantization of Chaos," *Physical Review Letters*, **67**, 15, October 1991 pp. 1941-1944.

P. Gaspard and D. Alonso, " Expansion for the Periodic-Orbit Quantization of Hyperbolic Systems," *Physical Review A*, **47**, 5, May 1993, pp. R3468-R3471.

Numerical Tools and Results (Section 4.2.2)

S. W. McDonald and N. A. Kaufman, "Spectrum and Eigenfunctions for a Hamiltonian with Stochastic Trajectories," *Physical Review Letters*, **42**, 18, April 1979, pp. 1189-1191.

M. V. Berry, "Quantizing a Classically Ergodic System. Sinai's Billiard and the KKR Method," *Annals of Physics*, **131**, 1, January 1981, pp. 163-216.

E. B. Bogomolny, "Semiclassical Quantization of Multidimensional Systems," *Nonlinearity*, **5**, 4, July 1992, pp. 805-866.

E. Doron and U. Smilanski, "Semiclassical Quantization of Chaotic Billiards – A Scattering Theory Approach," *Nonlinearity*, **5**, 5, September 1992, pp. 1055-1084.

E. Vergini and M. Saraceno, "Calculation by Scaling of Highly Excited States of Billiards," *Physical Review E*, **52**, 3, September 1995, pp. 2204-2207.

L. Kosztin and K. Schulten, "Boundary Integral Method for Stationary States of 2D Quantum Systems," *International Journal of Modern Physics C*, **8**, 2, 1997, pp. 293-325.

B. Li, M. Robnik, and B. Hu, "Relevance of Chaos in Numerical Solutions of Quantum Billiards," *Physical Review E*, **57**, 4, April 1998, pp. 4095-4105.

A. N. Kaufman, I. Kosztin, and K. Schulten, "Expansion Method for Stationary States in Quantum Billiards," *American Journal of Physics*, **67**, 2, February 1999, pp. 133-141.

Experimental Tools and Results (Section 4.2.2)

H.-D. Gräf, H. L. Harney, H. Lengeler, C. H. Lewenkopf, C. Rangacharyulu, A. Richter, P. Schardt, and H. A. Weidenmüller, "Distribution of Eigenmodes in a Superconducting Stadium Billiard with Chaotic Dynamics," *Physical Review Letters*, **69**, 9, August 1992, pp. 1296-1299.

H. Alt, H.-D. Gräf, H.L. Harney, R. Hofferbert, H. Lengeler, C. Rangacharyulu, A. Richter, and P. Schardt, "Superconducting Billiard Cavities with Chaotic Dynamics: An Experimental Test of Statistical Measure," *Physical Review E*, **50**, 1, July 1994, pp. R1-R4.

S. Deus, P. M. Koch, and L. Sirko, "Statistical Properties of the Eigenfrequencies Distribution of 3D Microwave Cavities," *Physical Review E*, **52**, 1, July 1995, pp. 1146-1155.

H. Alt, H.-D. Gräf, H. L. Harney, R. Hoffenbert, H. Lengeler, A. Richter, P. Schardt, and H. A. Weidenmüller, "Gaussian Orthogonal Ensemble Statistics in a Microwave Stadium Billiard with Chaotic Dynamics: Porter Thomas Distribution and Algebraic Decay of Time Correlations," *Physical Review Letters*, **74**, 1, January 1995, pp. 62-65.

H. Alt, C. Dembowski, H.-D. Gräf, R. Hofferbert, H. Rehfeld, A. Richter,R. Schuhmann, and T. Weiland, "Wave Dynamical Chaos in a Superconducting Three-Dimensional Sinai Billiard," *Physical Review Letters*, **79**, 6, August 1997, pp. 1026-1029.

H.-J. Stöckmann, "Microwave Studies of Chaotic Billiards and Disordered Systems," *Journal of Modern Optics*, **49**, 12, October 2002, pp. 2045-2059.

Eigenvalues in Regular vs. Ray-Chaotic Billiards (Section 4.3.1)

H. Weyl, "Uber die Abhängigkeit der Eigenschwingungen einer Membran von deren Begrenzung," *Journal Für Die Reine Und Angewandte Mathematik*, **141**, 1912, pp. 1-11.

C. E. Porter, *Statistical Theory of Spectra*, New York, Academic Press, 1965.

R. Balian and C. Bloch, "Distribution of Eigenfrequencies for the Wave Equation in a Finite Domain: I. Three-Dimensional Problem with Smooth Boundary Surface," *Annals of Physics*, **60**, 1970, pp. 401-447.

R. Balian and C. Bloch, "Distribution of Eigenfrequencies for the Wave Equation in a Finite Domain: II. Electromagnetic Field. Riemannian Spaces," *Annals of Physics*, **64**, 1971, pp. 271-307.

M. V. Berry, "Semiclassical Theory of Spectral Rigidity," *Proceedings of the Royal Society of London*, **A400**, 1985, pp. 229-251.

M. V. Berry and M. Robnik, "Semiclassical Level Spacings Where Regular and Chaotic Orbits Coexist," *Journal of Physics A*, **17**, 12, August 1984, pp. 2413-2421.

T. H. Seligman and J. J. M. Verbaarschot, "Quantum Spectra of Classically Chaotic Systems with Time Reversal Invariance," *Physics Letters A*, **108**, 4, April 1985, pp. 183-231.

T. Yukawa and T. Ishikawa, "Statistical Theory of Level Fluctuations," *Progress of Theoretical Physics Supplements*, **98**, 1989, pp. 157-172.

T. Prosen and M. Robnik, "Semiclassical Energy Level Statistics in Transition Region between Integrability and Chaos: Transition from Brody-Like to Berry-Robnik Behaviour," *Journal of Physics A*, **27**, 24, December 1994, pp. 8059-8077.

B. Li and M. Robnik, "Separating the Regular and Irregular Energy Levels and Their Statistics in Hamiltonian Systems with Mixed Classical Dynamics," *Journal of Physics A*, **28**, 17, September 1995, pp. 4843-4857.

P. J. Forrester, N. C. Snaith, and J. J. M. Verbaarschot, "Developments in Random Matrix Theory," *Journal of Physics A*, **36**, 12, March 2003, pp. R1-R10.

Eigenfunctions in Regular vs. Ray-Chaotic Billiards (Section 4.3.2)

E. B. Bogomolny, "Smoothed Wave Functions of Chaotic Quantum Systems," *Physica D*, **31**, 2, June 1988, pp. 169-189.

M. Feingold, R. G. Littlejohn, S. B. Solina, and J. S. Pehling, "Scars in Billiards: The Phase Space Approach," *Physics Letters A*, **146**, 4, May 1990, pp. 199-203.

T. M. Antonsen, Jr., E. Ott, Q. Chen, and R. N. Oerter, "Statistics of Wavefunction Scars," *Physical Review E*, **51**, 1, January 1995, pp. 111-121.

B. Eckhardt, U. Dörr, U. Kuhl, and H.-J. Stöckmann, "Correlations of Electromagnetic Fields in Chaotic Cavities," *Europhysics Letters*, **46**, 2, April 1999, pp. 134-140.

A. Abdi, H. Hashemi, and S. Nader-Esfahani, "On the PDF of a Sum of Random Vectors," *IEEE Transactions on Communications*, **48**, 1, January 2000, pp. 7-12.

Pulsed Problems (Section 4.3.3)

C. Draeger and M. Fink, "One-Channel Time Reversal of Elastic Waves in a Chaotic 2D-Silicon Cavity," *Physical Review Letters*, **79**, 3, July 1997, pp. 407-410.

C. Draeger and M. Fink, "One-Channel Time-Reversal in Chaotic Cavities: Theoretical Limits," *Journal of the Acoustical Society of America*, **105**, 2, February 1999, pp. 611-617.

C. Draeger and M. Fink, "One-Channel Time-Reversal in Chaotic Cavities: Experimental Results," *Journal of the Acoustical Society of America*, **105**, 2, February 1999, pp. 618-625.

R. A. Jalabert and H. M. Pastawski, "Environment-Independent Decoherence Rate in Classically Chaotic Systems," *Physical Review Letters*, **86**, 12, March 2001, pp. 2490-2493.

Introducing the Feature Article Authors

Vincenzo Galdi was born in Salerno, Italy, on July 28, 1970. He received the Laurea degree (*summa cum laude*) in Electrical Engineering and the PhD degree in Applied Electromagnetics from the University of Salerno, Italy, in 1995 and 1999, respectively.

From April to December, 1997, he held a visiting position in the Radio Frequency Division of the European Space Research & Technology Centre (ESTEC-ESA), Noordwijk, The Netherlands. From September, 1999, to August, 2002, he held a research associate position in the Department of Electrical and Computer Engineering at Boston University, Boston, MA. In November, 2002, he was appointed Associate Professor of Electromagnetics, and joined the Department of Engineering at the University of Sannio, Benevento, Italy, where he is currently working.

His research interests include analytical and numerical techniques for wave propagation in complex environments, electromagnetic chaos, and inverse scattering. Dr. Galdi was the recipient of a 2001 International Union of Radio Science (URSI) Young Scientist Award. He is a member of the IEEE and of Sigma Xi.

Innocenzo M. Pinto was born and educated in Italy. Winner of national competitions, he was appointed Assistant Professor of Electromagnetics in 1983, Associate Professor in 1987, and Professor in 1990. He has been a faculty member in the Universities of Naples, Salerno (where he founded and chaired the PhD program in Information Engineering from 1993-2001), Catania, and Sannio at Benevento, where he is currently the Dean of the Information Engineering Curricula Committee. He has visited several research institutions as an invited lecturer, including CERN, KEK, and NIST (former NBS). In 1998, he was an EU senior visiting scientist at the National Astronomical Observatory, Tokyo, Japan, in connection with the TAMA300 experiment.

Prof. Pinto has authored or co-authored more then 100 technical papers in peer-reviewed international journals. His research interests span electro-physics to gravitational wave experiments. He is a member of the IEEE and of the American Physical Society.

Leopold B. Felsen was born in Munich, Germany, on May 7, 1924. He received the BEE, MEE, and DEE degrees from the Polytechnic Institute of Brooklyn, Brooklyn, NY, in 1948, 1950, and 1952, respectively.

He emigrated to the United States in 1939 and served in the US Army from 1943 to 1946. After 1952, he remained with the Polytechnic (now Polytechnic University), gaining the position of University Professor in 1978. From 1974 to 1978, he was Dean of Engineering. In 1994, he resigned from the full-time Polytechnic faculty and was granted the status of University Professor Emeritus. He is now Professor of Aerospace and Mechanical Engineering and Professor of Electrical and Computer Engineering at Boston University, Boston, MA (part-time).

Dr. Felsen is the author or coauthor of over 350 papers and of several books, including the classic *Radiation and Scattering of Waves* (Piscataway, NJ, IEEE Press, 1994). He is an Associate Editor of several professional journals, and was an Editor of the *Wave Phenomena Series* (New York, Springer-Verlag). His research interests encompass wave propagation and diffraction in complex environments and in various disciplines, high-frequency asymptotic and short-pulse techniques, and phase-space methods with an emphasis on wave-oriented data processing and imaging.

Dr. Felsen is a member of Sigma Xi, a Life Fellow of the Institute of Electrical and Electronics Engineers, and a Fellow of the Optical Society of America and of the Acoustical Society of America. He has held named Visiting Professorships and Fellowships at universities in the United States and abroad, including the Guggenheim in 1973 and the Humboldt Foundation Senior Scientist Award in 1981. In 1974, he was an IEEE AP-S Distinguished Lecturer. His Poet's Corner appears sporadically in the *IEEE Antennas and Propagation Magazine*. Dr. Felsen received the IEEE AP-S Best Paper Award for 1969, and was Best Paper coauthor for 1974 and 1981; he was a contributing author to papers selected for the R. W. P. King Award for 1984, 1986, and 2000. He received the Balthasar van der Pol Gold Medal from the International Union of Radio Science (URSI) in 1975, an honorary doctorate from the Technical University of Denmark in 1979, the IEEE Heinrich Hertz Gold Medal for 1991, the AP-S Distinguished Achievement Award for 1998, the IEEE Third Millennium Medal in 2000 (nomination by AP-S), an honorary Laurea degree from the University of Sannio in Benevento, Italy, in 2003, the IEEE Electromagnetics Award for 2003, an honorary doctorate from the Technical University of Munich, Germany, in 2004, three Distinguished Faculty Alumnus Awards from Polytechnic University, and the IEEE Centennial Medal in 1984. In 1977, he was elected to the National Academy of Engineering. He served on the AP-S Administrative Committee from 1963-1966, and was Vice Chair and Chair for both USNC (1966-1973) and international (1978-1984) URSI Commission B.